Physics in Medicine & Biology

IPEM
Institute of Physics and
Engineering in Medicine

CrossMark

TOPICAL REVIEW

Measurement and image-based estimation of dielectric properties of biological tissues —past, present, and future—

Kensuke Sasaki[1] , Emily Porter[2], Essam A Rashed[3] , Lourdes Farrugia[4] and Gernot Schmid[5]

[1] National Institute of Information and Communications Technology, Tokyo, Japan
[2] Department of Electrical and Computer Engineering, The University of Texas at Austin, Austin, United States of America
[3] Graduate School of Information Science, University of Hyogo, Kobe, Japan
[4] Department of Physics, University of Malta, Msida, Malta
[5] Seibersdorf Labor GmbH, Seibersdorf, Austria

E-mail: k_sasaki@nict.go.jp

Abstract

The dielectric properties of biological tissues are fundamental parrameters that are essential for electromagnetic modeling of the human body. The primary database of dielectric properties compiled in 1996 on the basis of dielectric measurements at frequencies from 10 Hz to 20 GHz has attracted considerable attention in the research field of human protection from non-ionizing radiation. This review summarizes findings on the dielectric properties of biological tissues at frequencies up to 1 THz since the database was developed. Although the 1996 database covered general (normal) tissues, this review also covers malignant tissues that are of interest in the research field of medical applications. An intercomparison of dielectric properties based on reported data is presented for several tissue types. Dielectric properties derived from image-based estimation techniques developed as a result of recent advances in dielectric measurement are also included. Finally, research essential for future advances in human body modeling is discussed.

1. Introduction

Human interaction with electromagnetic fields, along with human protection, has been a long-standing topic in the field of biomedical engineering. In the international guidelines and standards for human protection (ICNIRP 2010, ICNIRP 2020a, IEEE-C95.1 2019), exposure limits have been prescribed for frequencies from 0 Hz to 300 GHz. In the frequency range below 100 kHz, electrostimulation due to the electromagnetic field is the dominant effect, and is thus applied to the neuromodulation. In the frequency range above 100 kHz, the heating or resultant temperature rise is the primary effect, and is thus applied to clinical applications, e.g. hyperthermia and radiofrequency ablation.

In modern bioelectromagnetic field modeling, an anatomical human body or body-part models are used to identify the induced (defined as 'internal' in ICNIRP and '*in situ*' in IEEE) electric field in the human body. Dielectric properties, i.e. permittivity and electrical conductivity, of biological tissues are fundamental parameters used to assess the interaction between the human body and electric, magnetic, and electromagnetic fields. Thus, the determination of dielectric properties has become an essential topic with the advances in computational approaches in this research fields.

Early reviews on the dielectric properties of general (normal) tissues were reported by Foster and Schwan (1989) and Gabriel *et al* (1996a). Coinciding with the publication of the review of Gabriel *et al* in 1996, a database consisting of measurement data (Gabriel *et al* 1996b) and empirical equations (Gabriel *et al* 1996c) for the dielectric properties of tissues was developed for the dosimetry of human exposure to electromagnetic fields. In addition to these papers, additional details of their achievements were summarized in a technical report (Gabriel 1996), and all measurement results and parametric models were included in an online document

Figure 1. Number of citations of dielectric properties of biological tissues from 1996 to 2021.
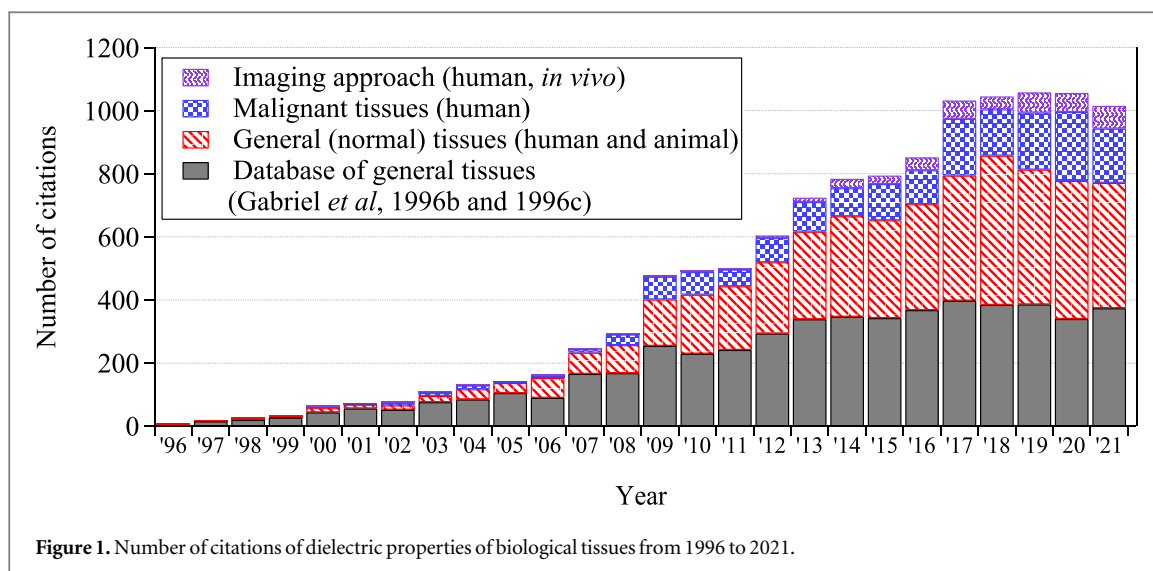
(Gabriel and Gabriel 1997). The total number of citations of the database (Gabriel *et al* 1996b, 1996c) has now reached 5200 (Web of Science, January 2022). This series of publications has contributed to substantial research and serves as a basis for widely used online resources concerning the dielectric properties of tissues (IFAC-CNR (1997), Hasgall *et al* (2015)). However, one limitation of the database is lack of the data for frequencies above 20 GHz as well as its inclusion of results from only a small number of papers that reported data below 1 MHz. With the emergence of wireless products utilizing these frequency domains (below 1 MHz and above 20 GHz), such as wireless transfer technology (Bi *et al* 2016, Rayes *et al* 2016) and mobile communication technologies (Watanabe *et al* 2021), and the interest in the variability in the electromagnetic modeling of the human body, the investigation of the dielectric properties of tissues is one of the key topics in the dosimetry of human exposure (SCENIHR 2009, 2015, Reilly and Hirata 2016, ICNIRP 2020b, Hirata *et al* 2021a, 2021b). Figure 1 shows the number of citations of research papers (cited in this review) on the dielectric properties of tissues from 1996 to 2021. Although the number of citations of the database (black bars in figure 1) is the largest, the number of citations of papers on other investigations of general (normal) tissues has also been increasing over time (red bars).

The dielectric properties of tissues are key parameters used in the design and optimization of many impedance-based and electromagnetic-based medical technologies. Early reviews on the use of dielectric properties for diagnostic and therapeutic medical applications focused on technologies for bone healing and hyperthermia treatment utilizing frequencies from 1 Hz to 10 GHz (Pethig 1984, Foster and Schwan 1989). With the advancement of technologies utilizing electromagnetic fields, a wide variety of applications have been proposed. Such applications include microwave and millimeter-wave imaging (Martellosio *et al* 2015), electrical impedance tomography (Li *et al* 2016), MR electrical property tomography (Li *et al* 2016), microwave ablation (O'Rourke *et al* 2007), and *in vitro* discrimination of pathological samples (Halter *et al* 2009). The underlying basis for such technologies is the fact that the dielectric properties often differ between diseased and healthy tissues, providing the opportunity to detect, diagnose, monitor, and treat diseases through methods that take advantage of this dielectric contrast. Moreover, the feasibility and efficacy of such technologies are also linked with the dielectric contrast. Knowledge of the dielectric properties of diseased (malignant) tissues is particularly vital for supporting studies on electromagnetic-based medical technologies for diagnosis, monitoring, and treatment of disease. To date, a relatively limited number of studies have provided data originating from measurements on human samples, which of course are of most interest for medical technologies. The dielectric properties of malignant tissues, as well as those of general (normal) tissues, have remained a topic of interest in this research area, and the number of citations of investigations focusing on malignant tissues (here of only human origin) has been increasing each year from 2000 (blue bars in figure 1).

With the advancement of imaging technologies such as MRI, non-invasive approaches for estimating dielectric properties have been proposed. In recent years, several approaches have been adapted to human subjects, and the number of citations has increased in the past decade (purple bars in figure 1). Although the number of citations has been relatively small compared with that of other topics, as can be seen in figure 1, these approaches have the potential to clarify the dielectric response of human tissues in the active state (e.g. physiological response) or the anisotropic response of the dielectric properties, bringing about new developments in the electromagnetic modeling of humans. Therefore, it is beneficial to outline the state-of-the-art and discuss future perspectives on the dielectric properties of tissues by considering the current status of

other research. The image-based estimation of dielectric properties has strong potential to progress with the emergence of machine learning techniques and big data analysis. The research in this direction is still in its early stages and is worth noting as a future perspective.

This review focuses on the dielectric properties of tissues up to THz frequencies that are beneficial for advances in research topics relevant to electromagnetic modeling of the human body. Related papers published in scientific journals were searched for systematically, and those published after 1996 were included in this review, considering the year of publication of the most cited review papers in the related research field. After summarizing the technical background in section 2, dielectric property data obtained *in vivo* or *in vitro/ex vivo* using excised tissue (hereinafter referred to as *in vitro*) on general (normal) and malignant tissues are summarized in sections 3 and 4, respectively. The measurement-specific factors that affect dielectric properties are described in section 5, and recent advances in estimating dielectric properties using imaging techniques are shown in section 6. Here, research items essential for future advances in the relevant research fields are also discussed on the basis of our review.

2. General descriptions of dielectric measurement

2.1. Metrics of dielectric properties

Different metrics of dielectric properties are often used in different frequency regions. In the radiofrequency region, permittivity (ε) [F/m] and electrical conductivity (σ) [S/m] are common physical quantities used to represent the dielectric response of materials. Also, relative permittivity (ε_r') or relative complex permittivity ($\varepsilon_r' - j\varepsilon_r''$) are used as dimensionless quantities (Foster and Schwan 1996);

$$\varepsilon_r' - j\varepsilon_r'' = \frac{\varepsilon}{\varepsilon_0} - j\frac{\sigma}{2\pi f\varepsilon_0}, \tag{1}$$

where ε_0 and f are the permittivity in vacuum (approximately 8.854×10^{-12} F m^{-1}) and frequency [Hz], respectively.

In the low-frequency domain, resistivity [Ω m], which is equivalent to σ^{-1}, is often used as a metric of dielectric measurement instead of conductivity (Foster and Schwan 1996).

At frequencies over 100 GHz, physical quantities of the optical domain, such as the refractive index (n), extinction coefficient (κ), and absorption coefficient (μ_a) [m^{-1}], are often used (Jacques 2013). For a non-magnetic medium, the relationships between these quantities are

$$n - j\kappa = (\varepsilon_r' - j\varepsilon_r'')^{1/2}, \tag{2}$$

$$\mu_a = \frac{4\pi\kappa}{\lambda_0}, \tag{3}$$

where λ_0 is the wavelength in a vacuum.

The scope of this review is the dielectric data of tissues at frequencies of up to 1 THz; therefore, there is a variety of metrics for the reported data depending on the area of expertise of the authors or the journal. To ensure consistency throughout this review, the relative permittivity and (electrical) conductivity are used as the common metrics unless otherwise stated.

2.2. Dielectric dispersions of biological tissues

There are three typical dielectric dispersion phenomena that determine the dielectric properties of tissues from extremely low frequencies to a few hundred GHz: α-, β-, and γ-dispersions (Schwan 1957, Foster and Schwan 1996). α-dispersion is observed at frequencies lower than 10 kHz and is considered to be related to the migration of cell ions in the tissue. The β-dispersion around the MHz band and the γ-dispersion around the GHz band are respectively due to interfacial polarization at the cell membrane interface in the tissue and to the rotation of the dipole moment of water molecules.

On the basis of these dielectric dispersion characteristics, the multiple dispersion is formulated using the empirical equation of the multipole Cole–Cole model, and this equation can be used for a computational approach;

$$\varepsilon_r'(f) - j\varepsilon_r''(f) = \varepsilon_\infty - j\frac{\sigma_{DC}}{2\pi f\varepsilon_0} + \sum_{i=1}^{N}\frac{\Delta_i}{1 + (jf/f_{r,i})^{1-\alpha_i}}, \tag{4}$$

where ε_∞ and σ_{DC} are the relative permittivity at $f \gg f_r$ and the DC conductivity [S/m], respectively. Δ_i, $f_{r,i}$, and α_i are the magnitude, generalized relaxation frequency [Hz], and distribution parameter, respectively, in the ith dispersion.

Table 1. Overview of review results concerning dielectric properties of skin tissues.

Author	Frequency	Tissues	Source	State	Tissue temperature
Gabriel *et al* (1996b, 1996c)	10 Hz–20 GHz	Dry skin and wet skin	Human (forearm)	*In vivo*	Not reported
Pickwell *et al* (2004)	0.1–3 THz	Epidermis	Human (forearm)	*In vivo*	Not reported
Alekseev and Ziskin (2007)	37–74 GHz	Stratum corneum (SC) and skin w/o SC layer	Human (palm and forearm)	*In vivo*	Not reported
Alekseev *et al* (2008)	37–74 GHz	Skin	Murine	*In vivo*	30 °C–33 °C
Karacolak *et al* (2009)	0.2–20 GHz	Skin	Rat	*In vitro*	38 °C
Chahat *et al* (2011)	10–60 GHz	Skin	Human (palm, wrist and thumb)	*In vivo*	30 ± 2 °C
Wilmink *et al* (2011)	0.13–1.6 THz	Skin	Porcine	*In vitro*	Not reported
Sasaki *et al* (2014a)	0.5–110 GHz	Epidermis and dermis	Porcine	*In vitro*	34 °C–37 °C
Zaytsev *et al* (2015)	0.3–1 THz	Skin	Human	*In vivo*	Not reported
Wake *et al* (2016)	10 kHz–1 MHz	Epidermis and dermis	Porcine	*In vitro*	35 °C
Sasaki *et al* (2017)	0.1–1 THz	Dermis	Porcine	*In vitro*	35 °C
Mirbeik-Sabzevari *et al* (2018)	0.5–50 GHz	Skin	Human	*In vitro*	22 °C
Zhekov *et al* (2019)	5–67 GHz	Dry skin and wet skin	Human (palm and thumb)	*In vivo*	Not reported

Since water is a major component of most tissues, the dielectric properties of water contents partly determine the dielectric properties of tissues (e.g. Gabriel *et al* 1996c). The dielectric properties of water depend on temperature within the frequency range in γ–dispersion; the relaxation frequency of pure water is in the range of 16–27 GHz at water temperatures of 20 °C–40 °C (Ellison 2007). This fact suggests that the dielectric properties of water in tissues have a strong temperature dependence in the frequency range of γ–dispersion (roughly in the range of 10–100 GHz). In addition, not only the γ-dispersion but also other dispersion characteristics of water may affect the dielectric properties of tissues. An empirical equation combining the multi-pole Debye model and the Lorentz model has been utilized for pure water for frequencies of up to approximately 30 THz (Liebe *et al* 1991, Ellison 2007). Although the multi-pole Debye model was utilized to formulate the dielectric properties of skin tissue at THz frequencies by Pickwell *et al* (2004), note that a Lorentz-type dispersion has the potential to be utlized to characterize the dielectric properties of tissues at frequencies around 1 THz.

2.3. Methods of dielectric measurement

Since tissues contain electrolytes, they have a high loss compared with low-loss (low-conductivity) materials such as antenna substrates of interest in the material measurement field. In addition, most tissues are flexible materials. Therefore, the coaxial probe (often referred to as the coaxial sensor) is the most frequently applied approach (Athey *et al* 1982, Gregory and Clarke 2006), particularly at radiofrequencies up to 100 GHz. Dielectric properties are derived from the measured impedance or reflection by representing the electromagnetic response by either analytical formulae (Mosig *et al* 1981) or equivalent circuit models (Stuchly *et al* 1982). Several sets of coaxial probes and methods to convert complex permittivities from the measurands have been developed (Stuchly and Stuchly 1980a, Gabriel *et al* 1994, Berube *et al* 1996, Sasaki *et al* 2018). Recently, a review of procedures for the dielectric measurement of tissues and guidance for the measurement processes has been made by La Gioia *et al* (2018).

In dielectric measurements at frequencies below 10 MHz, the use of a pair of electrodes is a fundamental technique (Yamamoto and Yamamoto 1976). In addition, different probe types, such as two-terminal (electrode) probes and coaxial probes, have been adopted in dielectric measurements. In this frequency range, care should be taken to account for electrochemical phenomena, referred to as electrode polarization, i.e. the generation of an electric double layer due to the accumulation of electrolytes in the tissues at the boundary between the electrode interface and tissues. The electrode polarization effect increases with decreasing frequency and depends on the dielectric properties of tissues, the mechanical dimensions, and the materials of the electrodes (Kuang and Nelson 1998). Compensation measurement methods such as the four-electrode method, which correct for electrode polarization and thereby suppress its influence, have been proposed (Schwan and Ferris 1968) and utilized for the dielectric measurement of tissues (e.g. Plonsey and Barr (1982)).

There have been few studies of the dielectric measurement of tissues at frequencies over 100 GHz. Tissues contain water, therefore the penetration depth becomes shallow over 100 GHz; the penetration depth of skin is below 0.4 mm at frequencies over 100 GHz (ICNIRP 2020a). Thus, methods based on reflection measurement,

which utilize free-space as a transmission line instead of a coaxial line or waveguide and use time-domain spectroscopy (TDS), are adopted for the dielectric measurement of tissues (Mirabella 1993, Pickwell *et al* 2004).

An image-based estimation method of dielectric properties refferred to as electrical properties tomography (EPT) enables the non-invasive acquisition of dielectric properties. Therefore, it may provide a more accurate estimation of the spatial distribution of dielectric properties considering subject/tissue variabilities attributed to water/ionic concentrations. Images of the dielectric properties are generated through a reconstruction method based on Maxwell's equations with a standard MRI scanner. Image-based methods are known to have good potential for imaging abnormal tissues such as tumours with superior resolution in many clinical applications (Liu *et al* 2017).

3. Dielectric characterization of general biological tissues

A systematic search of the literature reporting the dielectric measurements of general (normal) tissues, which have not been classified as malignant or benign, was conducted using Web of Science (August 2021); details of the search terms are given in appendix A. The measurements of human and animal subjects are the scope of this section, while studies on dielectric measurement with image-based estimation method are separately discussed in section 6. Review results for specific tissues, i.e. skin, adipose, and brain tissues, are summarized in sections 3.1 to 3.3, respectively, including comparisons between reported data. In addition, investigations focusing on the anisotropy of muscle tissue are summarized in section 3.4, and dielectric measurements for other tissues were summarized in section 3.5. Finally, a discussion is given and the research studies needed are highlighted in section 3.6.

3.1. Skin

3.1.1. Review

Summaries of the 13 papers presenting dielectric measurements of skin and/or the tissues composing skin listed in table 1 are provided below.

Gabriel *et al* (1996b) measured the dielectric properties of human skin (forearm) *in vivo* from 10 Hz to 20 GHz. Measurements were conducted using three different coaxial probes to cover this wide frequency range. On the basis of these measurements and their review (Gabriel *et al* 1996a), parametric models for dry and wet skin were developed using the four-pole Cole–Cole model (Gabriel *et al* 1996c). Relevant differences in the dispersion characteristics between dry and wet skin were only observed below 100 MHz, which is due to the absence of α- and β-dispersions for dry skin. Moreover, this also indicates that the stratum corneum predominantly determines the measurement results for skin (Gabriel 1997).
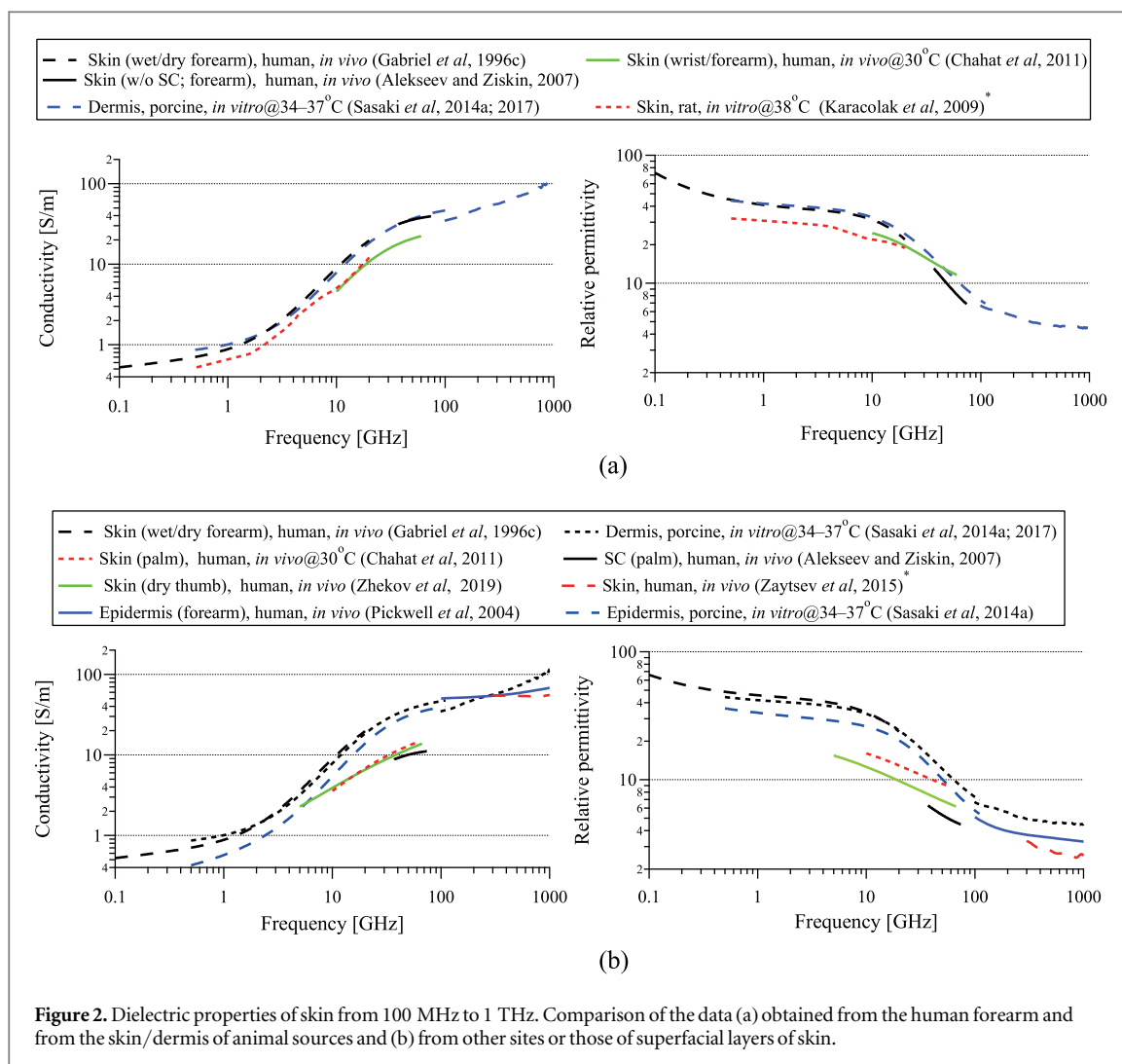
Pickwell *et al* (2004) measured the THz response of human skin *in vivo* using THz-TDS. THz responses of the palm and/or forearm were measured for 20 volunteers. Dielectric properties of the epidermis were estimated from the obtained mean response from measurements at the forearm of 18 volunteers (24–49 years of age) and a corresponding parametric model was reported using a two-pole Debye model.

Alekseev and Ziskin (2007) measured the dielectric properties of the tissues constituting human skin *in vivo* from 37 to 74 GHz using open-ended waveguides. The dielectric properties of the stratum corneum and the other skin layers, i.e. the epidermis and dermis without the stratum corneum, were estimated from measurements at the palm and forearm of 12 volunteers (45–60 years of age). Parametric models of each skin layer were reported for the palm and forearm. It was found that the skin water content is the dominant factor for determining the dielectric properties of skin in the considered frequency range.

Alekseev *et al* (2008) measured murine skin *in vivo* at frequencies from 37 to 74 GHz. The effect of body hair on the measured dielectric properties was investigated using hairy and hairless mice. Their results showed that the presence of hair led to slightly (5%–14%) lower dielectric properties than those of hairless skin. However, this difference was considered marginal by the authors as the results were within the measurement uncertainty of 10%.

Karacolak *et al* (2009) measured rat skin *in vitro* from 200 MHz to 20 GHz at 38 °C for the purpose of designing an implantable antenna. Parametric models using two- and three-pole Cole–Cole models were also presented.

Chahat *et al* (2011) measured the complex permittivity of human skin *in vivo* from 10 to 60 GHz using a coaxial probe. The measurements were performed at several body parts, i.e. the palm, wrist, and forearm, for each of seven volunteers. The obtained results for the wrist and forearm were in good agreement, i.e. the observed differences were within the spread expected for this kind of measurement. However, the measurement results obtained at the palm tended to be lower than those at the wrist and forearm, which can be explained by the difference in the thickness of the stratum corneum, which has a low water content. Also, parametric models were reported for the wrist/forearm and palm.

Figure 2. Dielectric properties of skin from 100 MHz to 1 THz. Comparison of the data (a) obtained from the human forearm and from the skin/dermis of animal sources and (b) from other sites or those of superfacial layers of skin.

Wilmink *et al* (2011) reported the optical properties, i.e. refractive index and absorption coefficient, of porcine skin *in vitro* from 0.13 to 1.6 THz at room temperature using THz-TDS. The presented results were compared with those measured by Pickwell *et al* (2004), and the discrepancies were within 15% and 40% for the diffraction index and absorption coefficients, respectively.

Sasaki *et al* (2014a) measured the dielectric properties of skin tissues, i.e. the epidermis and dermis, of porcine skin from 0.5 to 110 GHz at 34 °C–37 °C. Coaxial probe and free-space methods were adopted for the dielectric measurement, and parametric models using the two-pole Cole–Cole model were also reported. Their results for porcine dermis at frequencies up to 20 GHz were in good agreement with the dielectric properties for dry human skin obtained by Gabriel *et al* (1996c) *in vivo*. This observation remains interesting, because the data obtained at the surface of dry skin by Gabriel *et al* (1996b, 1996c) were expected to be predominantly determined by the dermis up to 20 GHz (Gabriel 1997).

Zaytsev *et al* (2015) investigated the dielectric properties of human skin *in vivo* from 0.3 to 1 THz using THz-TDS for a purpose of diagnosis application. The dielectric properties of healthy skin and dysplastic and non-dysplastic skin nevi were measured from four patients.

Wake *et al* (2016) reported conductivities of the porcine epidermis and dermis *in vitro* at 35 °C from 10 kHz to 1 MHz using a two-electrode method. The conductivities of epidermis were estimated from bulk skin comprising the epidermis and dermis. The measured conductivities of the dermis were almost constant in the considered frequency range, while those of the epidermis showed frequency-dependent characteristics. The authors found that the conductivities of both the epidermis and dermis contribute to the overall conductivity of skin, i.e. both the epidermis and dermis should be considered in numerical models.

Sasaki *et al* (2017) measured the dielectric properties of porcine dermis *in vitro* at 35 °C from 0.1 to 1 THz using THz-TDS. The obtained data showed reasonable agreement (within 8% and 25% deviations for permittivity and conductivity, respectively) with the data obtained by Sasaki *et al* (2014a) at 100 GHz with a different measurement methodology (see above).

Table 2. Overview of review results for adipose tissue.

Author	Frequency	Tissues	Source	State	Tissue temperature
Gabriel *et al* (1996b, 1996c)	10 Hz–20 GHz	Adipose tissue	Human, ovine, and bovine Porcine	*In vitro*	37 °C
					20 °C
Lazebnik *et al* (2007a)	50 MHz–20 GHz	Breast tissue	Human (reduction surgery)	*In vitro*	18 °C–26.6 °C
Lazebnik *et al* (2007b)	50 MHz–20 GHz	Breast tissue	Human (cancer surgery)	*In vitro*	18 °C–27.2 °C
Stoneman *et al* (2007)	40 Hz–100 MHz	Adipose tissue	Human	*In vitro*	37 °C
Bindu and Mathew (2008)	2.4–3.0 GHz	Breast tissue	Human	*In vitro*	Not reported
Gabriel *et al* (2009)	40 Hz–1 MHz	Fat	Porcine	*In vivo*	37 °C
Ashworth *et al* (2009)	0.15–2 THz	Fat and fibrous tissues	Human	*In vitro*	Not reported
Wilmink *et al* (2011)	0.13–1.6 THz	Adipose tissue	Porcine	*In vitro*	Not reported
Sugitani *et al* (2014)	0.5–20 GHz	Breast tissue	Human	*In vitro*	18 °C–24.1 °C
Martellosio *et al* (2015)	0.5–50 GHz	Breast tissue	Human	*In vitro*	25 °C
Wake *et al* (2016)	10 kHz–1 MHz	Subcutaneous tissue	Porcine	*In vitro*	35 °C
Martellosio *et al* (2017)	0.5–50 GHz	Breast tissue	Human	*In vitro*	19 °C–22 °C
Sasaki *et al* (2017)	1 GHz–1 THz	Subcutaneous tissue	Porcine	*In vitro*	35 °C

Mirbeik-Sabzevari *et al* (2018) measured human skin *in vitro* at frequencies from 0.5 to 50 GHz using a coaxial probe. The measurement was conducted at room temperature of 22 °C. Normal and malignant skin were collected by surgery from 41 patients aged 34–89. Single-pole Cole–Cole models for each tissue were reported. The obtained results for normal skin showed agreement within 10% difference from those of wet skin reported by Gabriel *et al* (1996c). The authors also observed large variability between the patients' subgroups as compared with the samples within each patient subgroup. However, according to the authors, this was expected as the tissues were excised from different body locations for different patients.

Zhekov *et al* (2019) reported the dielectric properties of human hands obtained *in vivo* from 5 to 67 GHz using a coaxial probe. Palms and thumbs under dry and moist conditions were measured for 22 volunteers. In addition, parametric models for each part and condition were derived using a single-pole Cole–Cole model. The difference in permittivity between dry thumbs and palm was within 10%. For the conductivity, similar differences of up to approximately 10% were observed in the frequency range up to approximately 20 GHz, which increased to up to 27% difference at higher frequencies. According to the authors, these observations are a consequence of the skin structure. Moreover, the authors noted significant variation in the dielectric properties among the test persons.

3.1.2. Comparison

Only two papers have reported dielectric measurements of skin frequencies below 500 MHz: Gabriel *et al* (1996b) reported measurements on the surface of intact dry and wet human skin, and Wake *et al* (2016) reported the results of in vitro measurements on porcine epidermis and dermis. The conductivity of the dermis obtained by Wake *et al* (2016) was almost constant at around 0.4 S m^{-1}, while the conductivity of the epidermis increased from 0.0036 to 0.12 S m^{-1} with increasing frequency from 10 kHz to 1 MHz. Although the frequency trend of epidermal conductivity is different from that of dry or wet skin reported by Gabriel *et al* (1996b), the values for the conductivity of wet skin reported by Gabriel *et al* (1996c) are within the range of those for the epidermis and dermis from 10 kHz to 1 MHz reported by Wake *et al* (2016). Gabriel *et al* (1996b) measured human skin (forearm) *in vivo* by contacting a coaxial probe on the skin surface, and thus the measurement results may reflect the differences in dieletric properties of different skin layers such as stratum corneum, epidermis, dermis, and subcutaneous tissue layers (Lahtinen *et al* 1997, Gabriel 1997). However, the fact that the permittivity data reported by Gabriel *et al* (1996b, 1996c) for dry skin did not show any α- or β-dispersion but some dispersion became visible after moistening the skin (data for wet skin in Gabriel *et al* (1996b, 1996c)), strongly suggests that the data for dry skin reported by Gabriel *et al* (1996b, 1996c) mainly reflect the dielectric properties of the stratum corneum in the low-frequency range. Also, Schmid *et al* (2013) pointed out the possibility that the stratum corneum, which has extremely low conductivity (Yamamoto and Yamamoto 1976), strongly affected the data for skin reported by Gabriel (1996). Similarly, Wake *et al* (2016) commented that the conductivity of dry skin reported by Gabriel (1996c) is in good agreement with that of the stratum corneum at 100 kHz, and did not practically represent the values of inner layers, the stratum granulosum layer or the deeper layer of epidermis and dermis.

Figure 2 shows a comparison of the dielectric properties of skin tissues between the measurements above 100 MHz. The authors of several studies in which dielectric measurements of skin were conducted *in vivo* reported that the considerable variability of the measured data with the body site can be attributed to the variability in skin layer thickness. Therefore, a comparison of the data obtained *in vivo* from the human forearm and those obtained from the skin/dermis of animal sources is given in figure 2(a), and a comparison of the data of human skin obtained from other sites (including those from reports where no site is mentioned) or those of superfacial layers of skin (stratum corneum and epidermis) is given in figure 2(b). The plots in figure 2 are of the original data or are derived from previously reported empirical equations, while for a few cases, plots were reproduced from figures in the original reference using *Engauge Digitizer ver. 12.1*. Note that data measured *in vitro* without the tissue temperature being reported and data measured at room temperature are excluded.

Figure 2(a) shows that although the source and measurement state were different between Gabriel *et al* (1996c) and Sasaki *et al* (2014a, 2017), both the conductivity and permittivity of human skin (forearm) measured *in vivo* and porcine dermis measured *in vitro* were in good agreement, with a difference of around 10%. The result of *in vitro* measurement of the dermis also agreed with the *in vitro* measurement result of human skin (without the stratum corneum layer) reported by Alekseev and Ziskin (2007). On the other hand, dielectric values for rat skin reported by Karacolak *et al* (2009) were approximately 30% lower than those reported by Gabriel *et al* (1996c). This difference is assumed to be acceptable because similar differences were observed between *in vivo* measurement results of human skin by Gabriel *et al* (1996c) and Chahat *et al* (2011).

The measurement results of human skin at several different sites shown in figure 2(b) present larger variations than the difference between the *in vivo* and *in vitro* measurements. The dielectric values of skin measured at the palm and thumb were 20%–70% lower than those obtained from porcine dermis by Sasaki *et al* (2014a). The dielectric properties of the palm and thumb measured *in vivo* were within the range of those of the epidermis and stratum corneum reported by Sasaki *et al* (2014a) and Alekseev and Ziskin (2007), respectively, above 40 GHz, but they tended to converge to the dielectric properties of the epidermis as the frequency decreased to 5 GHz. These observations suggest that the sensing depth for the measurement of the human palm was up to the epidermis layer and that the stratum corneum became the dominant layer at high frequencies in their measurements. At frequencies above 300 GHz, the results of *in vivo* measurements of the conductivity and permittivity of skin by Zaytsev *et al* (2015) were within 20% and 30% of those of the epidermis measured by Pickwell *et al* (2004), respectively. Although their target tissues were different, it is difficult to clarify the reason for the difference because Zaytsev *et al* (2015) did not report the body site of their *in vivo* measurement of human skin. In particular, at sub-millimeter-wave frequencies, variations in the thicknesses of the skin tissues are expected to strongly impact the measured dielectric properties of skin because of the shallow penetration depth.

3.2. Adipose tissue
3.2.1. Review
Summaries of the 13 papers presenting dielectric measurements of adipose tissue listed in table 2 are provided below.
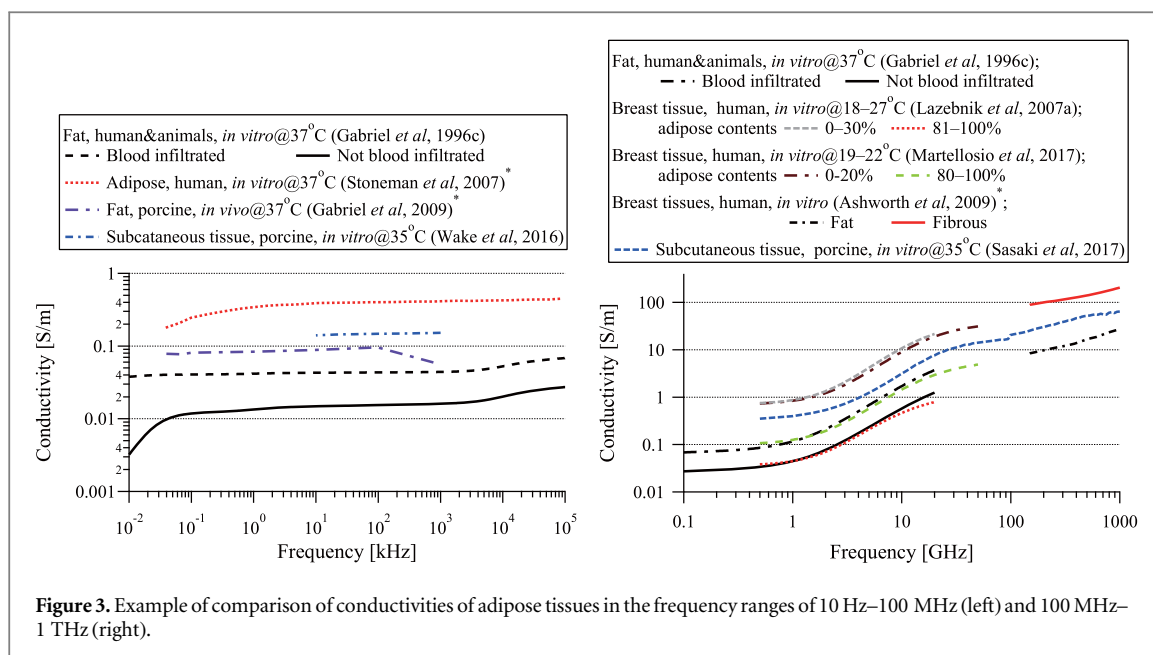
Gabriel *et al* (1996b) measured the dielectric properties of adipose tissue *in vitro* at body temperature using coaxial probes. Their results demonstrated a wide spread of dielectric properties between those obtained from humans and three animal origin, i.e. ovine, bovine, and porcine. They also distinguished between adipose tissue of high fat content (or low water content) and of the higher water content with blood infiltration. On the basis of these findings, two types of parametric models of fat, blood-infiltrated and non-infiltrated, were developed using a four-pole Cole–Cole model (Gabriel *et al* 1996c).

Lazebnik *et al* (2007a) measured human breast tissue *in vitro* between 50 MHz and 20 GHz using a coaxial probe. Tissue samples were obtained from 93 patients (17–65 years of age) by reduction surgery. Tissue temperatures during measurements were approximately from 18 to 26.6 °C. Very large variations (by a factor of 10 or larger) in dielectric properties were observed, and it was found that the dielectric properties were primarily determined by the adipose content of the tissues. Parametric models of the tissue categorized into three groups, i.e. low, middle, and high adipose contents, were also provided. In addition, the parametric models were improved to present better agreement with their measurement results in a later work (Lazebnik *et al* 2007c).

In a later study by Lazebnik *et al* (2007b), human breast tissue obtained from 196 patients (19–90 years of age) by cancer surgery were measured *in vitro* between 50 MHz and 20 GHz using a coaxial probe. Similarly to their previous study (Lazebnik *et al* 2007a), very large variations were observed between each sample, and it was found that the dielectric properties of tissues with low and high adipose contents obtained by cancer and reduction surgeries were in good agreement.

Stoneman *et al* (2007) measured the dielectric properties of human adipose tissue *in vitro*, obtained by surgical mastectomy, from 40 Hz to 100 MHz at approximately 37 °C using a coaxial probe. Tissue samples of

Figure 3. Example of comparison of conductivities of adipose tissues in the frequency ranges of 10 Hz–100 MHz (left) and 100 MHz–1 THz (right).

normal and cancerous breast tissues were obtained from 34 patients in total by surgical mastectomy. A parametric model proposed by Raicu (1999) was adopted and parametrized.

Bindu and Mathew (2008) reported the dielectric properties of human breast tissue *in vitro* from 2.4 to 3.0 GHz, measured using a rectangular cavity resonator. Tissue samples were obtained from six patients by an excisional surgical procedure. The bound water contents of the normal adipose tissues ranged from 41% to 49%.

Gabriel *et al* (2009) reported the conductivities of porcine fat *in vivo* at approximately 37 °C from 40 Hz to 1 MHz as a supplement of their database (Gabriel *et al* 1996b; 1996c). The dielectric measurement of the tissue was conducted using the four-electrode method. Their conductivities for fat were around twice those of the blood-infiltrated fat measured by Gabriel *et al* (1996c).

Ashworth *et al* (2009) measured the dielectric properties of human breast tissue *in vitro* at room temperature from 0.15 to 2 THz using THz-TDS. Tissue samples collected from 20 patients by breast conserving surgery were histologically separated into healthy adipose and fibrous tissues and breast cancer tissues. Parametric models were reported in a later work by Truong *et al* (2015).

Wilmink *et al* (2011) reported the optical properties, i.e. refractive index and absorption coefficient, of porcine adipose tissue *in vitro* from 0.13 to 1.6 THz at room temperature using THz-TDS. The measured results were compared with those of other groups. Up to 40% larger diffraction indexes were observed, and the absorption coefficients were two to ten times the values previously reported. The authors commented that a possible cause of the disagreement was the difference in the hydration state of the tissue in each study.

Sugitani *et al* (2014) reported the dielectric properties of human breast tissues (cancer, stroma, and adipose tissues) from 0.5 to 20 GHz *in vitro* using a coaxial probe for the purpose of microwave diagnostic application. The tissue samples were obtained from cancer surgeries of 35 patients of age 33–88 years. The dielectric measurements were conducted at temperatures of 18 °C–24.1 °C. Parametric models using a two-pole Cole–Cole model were also reported.

Martellosio *et al* (2015) measured the dielectric properties of human breast tissue *in vitro* at room temperature of 25 °C from 0.5 to 50 GHz using a coaxial probe. The normal and malignant tissues were obtained by surgery. Parametric models using a single-pole Cole–Cole model were also reported, and the results were in good agreement with those of edible fat.

Wake *et al* (2016) measured the conductivities of subcutaneous tissue (abdomen) of porcine *in vitro* at 35 °C from 10 kHz to 1 MHz using the two-electrode method. Their results were almost constant in the considered frequency range. The measured conductivity was six times that of fat reported by Gabriel *et al* (1996b, 1996c). Differences in the water contents of the tissue samples measured were reported to be the most likely cause of the difference.

Martellosio *et al* (2017) measured the dielectric properties of human breast tissue (obtained by cancer surgery) *in vitro* at 19 °C–22 °C from 0.5 to 50 GHz using a coaxial sensor. Large variations in the dielectric properties of normal breast tissue were reported, which were due to the large variation in tissue density (adipose content). Single-pole Cole–Cole models for different fat contents in three groups, i.e. low (80%–100% adipose contents), medium (20%–80% adipose contents), and high (0%–20% adipose contents) densities, were

Table 3. Overview of review results for brain tissue.

Author	Frequency	Tissues	Source	State	Tissue temperature
Gabriel *et al* (1996b, 1996c)	10 Hz–20 GHz	Grey matter and white matter	Ovine	*In vitro*	37 °C
Baumann *et al* (1997)	10 Hz –10 kHz	Cerebrospinal fluid	Human	*In vitro*	25 °C and 37 °C
Bao *et al* (1997)	45 MHz–26.5 GHz	Grey matter White matter	Rat	*In vitro*	24 °C and 37 °C 25 °C and 37 °C
Latikka *et al* (2001)	50 kHz	Cerebrospinal fluid, grey matter, and white matter	Human	*In vivo*	Not reported
Tofighi and Daryoush (2002)	15–50 GHz	Grey matter and white matter	Rat	*In vitro*	27 °C
Schmid *et al* (2003a)	0.9 and 1.8 GHz	Grey matter	Porcine	*In vivo* and *in vitro*	22 °C–39 °C
Schmid *et al* (2003b)	0.8–2.45 GHz	Grey matter	Human	In vitro	18 °C–25 °C
Peyman *et al* (2007)	50 MHz–20 GHz	Arachnoid, cerebrospinal fluid, dura mater, dura spinal cord, grey matter and white matter	Porcine	*In vivo* and *in vitro*	37 °C
Schmid *et al* (2007)	0.4–6 GHz	Pineal gland	Human	*In vitro*	18 °C
Gabriel *et al* (2009)	40 Hz–1 MHz	Cerebrospinal fluid	Porcine	*In vitro*	37 °C
Mohammed *et al* (2016)	0.3–3 GHz	Cerebrospinal fluid, grey matter and white matter	Canine	*In vitro*	Not reported

reported. The effects of the patient age, the sample temperature, and the time between excision and measurements were also discussed (overview were made in section 5).

Sasaki *et al* (2017) measured the dielectric properties of porcine subcutaneous tissue *in vitro* at 35 °C from 1 GHz to 1 THz using a coaxial probe and THz-TDS. The obtained results were compared with those of fat reported by Gabriel (1996) for frequencies up to 20 GHz. Their permittivity and conductivity values were up to three and seven times higher than those reported by Gabriel (1996) at frequencies up to 20 GHz, and differences in the water contents of the tissue samples were assumed as the cause of the large difference.

3.2.2. Comparison

The large spread of data can be attributed to the variation in the composition of adipose tissue as shown by several authors (Lazebnik *et al* 2007a, Martellosio *et al* 2017). Figure 3 shows examples of the conductivities of adipose tissues up to (left) and above (right) 100 MHz. The plots in the figure 3 are from the original data or derived from reported empirical equations, while for a few cases, plots were reproduced from figures in the original reference using Engauge Digitizer ver. 12.1.

At frequencies below 100 MHz, the spread of the conductivity values reported for adipose tissues is within a factor of 30 (maximum to minimum ratio). At frequencies from 100 MHz to 50 GHz, the spreads of the conductivity and permittivity values reported for adipose tissues are within factors of around 30 and 10, respectively. Note that several data were obtained using tissues at temperatures lower than body temperature (approximately 37 °C); however, the observed range of the spread cannot be explained only by temperature differences, as reported in previous investigations (see appendix B). The dielectric properties of fat (not infiltrated) reported by Gabriel *et al* (1996c) are in good agreement with those of breast tissue with high adipose contents (81%–100%) as reported by Lazebnik *et al* (2007a), and these values for permittivity and conductivity are considered as lower limits for adipose tissue. The values for tissue with low adipose contents (0%–20%) reported by Martellosio *et al* (2017) are assumed as the upper limit of the dielectric properties of adipose tissue up to 50 GHz. These observations demonstrated that adipose or water content is dominant factor determining large variations in the dielectric properties of adipose tissues. At frequencies above 50 GHz, the spread of values between the four studies were within factors of around 10 and 3 for conductivity and permittivity, respectively.

3.3. Brain tissues

3.3.1. Review

Summaries of the 11 papers presenting dielectric measurements of brain tissues listed in table 3 are provided below.

Gabriel *et al* (1996c) reported parametric models for ovine[6] grey and white matter *in vitro* at 37 °C based on their measurement from 10 Hz to 20 GHz (Gabriel *et al* 1996b). Authors demonstrated consistency between the frequency trends of the dielectric properties in their results and in previous studies reviewed by Gabriel *et al* (1996a).

Baumann *et al* (1997) measured the conductivity of human cerebrospinal fluid *in vitro* from 10 Hz to 10 kHz at 25 and 37 °C, using a four-electrode method. The measured samples were obtained from seven patients. Their results showed good agreement with those obtained from rabbit at 1 kHz.

Bao *et al* (1997) measured the dielectric properties of rat white and grey matter *in vitro* from 45 MHz to 26.5 GHz at 25 °C (or 24 °C) and 37 °C using a coaxial probe. Parametric models based on their measurement results were also reported.

Latikka *et al* (2001) measured the resistivity of human brain tissues, i.e. white matter, grey matter, and cerebrospinal fluid, *in vivo* at 50 kHz using a monopolar needle electrode, i.e. equipment usually used for pain treatment. The numbers of patients were five, eight, and two for white matter, grey matter, and cerebrospinal fluid, respectively, and the patients' age ranged from 32 to 87 years. They found that the mean values of conductivity (the inverse of resistivity) of grey matter was approximately 10% larger than that of white matter. In addition, they observed decreasing conductivity for grey matter during the operation.

Tofighi and Daryoush (2002) measured rat white and grey matter *in vitro* from 15 to 50 GHz at 27 °C using a microstrip line test fixture. Parametric models of tissues using the single-pole Cole–Cole model were also reported.

Schmid *et al* (2003a) measured the postmortem changes of the dielectric properties of grey matter of porcine brain at 0.9 and 1.8 GHz using a coaxial probe. The number of considered animals was 10, and both *in vivo* and *in vitro* measurements of the tissues were conducted. The results demonstrated that *in vitro* measurements of dielectric properties of brain tissue underestimate *in vivo* dielectric properties (detail of postmortem effect was summarized in 5.1).

---

[6] Tissue origin is noted as bovine in the figure caption of figure 2 of Gabriel *et al* (1996b), while in the text of the publication ovine is stated as the tissue origin. In this topical review we use 'ovine' instead of 'bovine' when referring to the tissue origin of figure 2 of Gabriel *et al* (1996b).
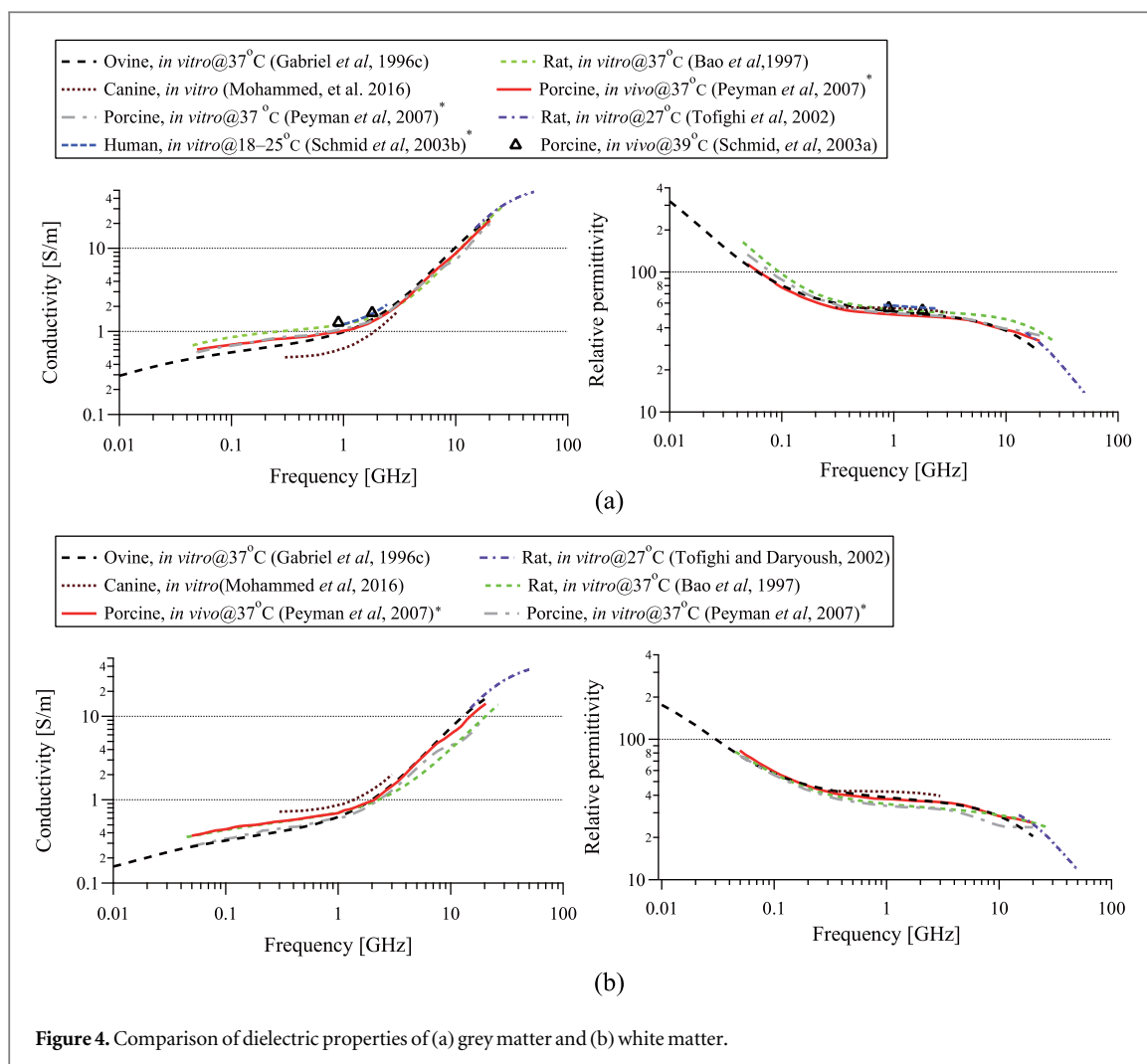
Figure 4. Comparison of dielectric properties of (a) grey matter and (b) white matter.

Schmid *et al* (2003b) reported the dielectric properties of human grey matter *in vitro* from 0.8 to 2.45 GHz at room temperature (18 °C–25 °C) using a coaxial probe. In total, 20 brains excised less than 10 h postmortem from the bodies of persons who died at ages between 47.5 and 87.5 years were investigated. The dielectric properties of human grey matter showed higher values compared to those reported by Gabriel *et al* (1996b) for human (24–48 h postmortem) and ovine (2 h postmortem) brain samples *in vitro* at body temperature. The authors also commented that the discrepancy from the values reported by Gabriel *et al* (1996b) for around 1 GHz was approximately 10%–30% when the technique used to adjust the tissue temperature from their former work (Schmid *et al* 2003a) using porcine brain was adopted.

Peyman *et al* (2007) measured porcine cerebrospinal tissues, i.e. arachnoid, grey matter, white matter, dura mater, and dura spinal cord, *in vivo* from 50 MHz to 20 GHz using a coaxial probe. In addition, the dielectric properties of these five tissues and cerebrospinal fluid were measured *in vitro* at 37 °C and their aging effect was also measured and discussed. Details of the comparison between *in vivo* and *in vitro* measurements and the aging effect are given in sections 5.1 and 5.3, respectively. The dielectric properties of porcine grey and white matter obtained *in vivo* showed good agreement with those obtained from ovine *in vitro* by Gabriel *et al* (1996b, 1996c), although they were somewhat lower than those reported by Bao *et al* (1997) and Schmid *et al* (2003a, 2003b). The authors commented that the differences in the tissue preparation process between the different studies were a possible cause of the discrepancy.

Schmid *et al* (2007) measured the dielectric properties of human pineal gland *in vitro* at frequencies ranging from 0.4 to 6 GHz at 18 °C using a coaxial probe. Tissue samples were obtained from 20 patients (26–91 years of age). The obtained data were used for computational simulations of electromagnetic field absorption.

Gabriel *et al* (2009) measured the conductivities of porcine cerebrospinal fluid *in vitro* at approximately 37 °C from 40 Hz to 1 MHz using a four-electrode method to supplement their database (Gabriel *et al* 1996b; 1996c).

Table 4. Overview of review results concerning measurements focusing on muscle anisotropy.

Author	Frequency	Muscle sites	Source	State	Maximum to minimum ratio due to anisotropy	
					Permittivity	Conductivity
Gabriel *et al* (1996b)	10 Hz–20 GHz	Not reported	Ovine	*In vitro*	Up to 5	Up to 1.5
Gabriel *et al* (2009)	40 Hz–1 MHz	Skeletal	Porcine	*In vivo*	Not measured	1.2–1.9
Ahad *et al* (2009)	2 kHz–1 MHz	Skeletal	Rat	*In vitro*	Around 1	1.3–3.6
Sanchez *et al* (2014)	1 kHz–10 MHz	Soleus and gastrocnemius	Rat	*In vivo*	Not measured	Up to 5.6
						Up to 3.0
Kwon *et al* (2019)	30 kHz–1 MHz	Skeletal	Ovine	*In vitro*	Not measured	Up to 1.2

Mohammed *et al* (2016) measured the dielectric properties of canine brain tissues, i.e. white matter, grey matter, and cerebrospinal fluid, *in vitro* at room temperature from 0.3 to 3 GHz using a coaxial probe. The aging effect on the dielectric properties was also investigated and discussed (details are shown in 5.3).

3.3.2. Comparison

The reported dielectric properties for grey and white matter are compared. Note that data are scarce below 45 MHz and above 50 GHz. Excluding the values reported by Gabriel *et al* (1996b, 1996c, 2009), the only values for brain tissue conductivity at 50 kHz were reported by Latikka *et al* (2001). The conductivity values reported by Latikka *et al* (2001) were 2.2 and 3.3 times those reported by Gabriel *et al* (1996c) for grey and white matter, respectively. Although the conditions of dielectric measurement, e.g. tissue source, state, and temperature, were different between the two studies, Gabriel *et al* (1996b) commented that the uncertainty in their measurement may be up to a factor of 2 or 3 due to the effect of electrode polarization below 100 Hz. On the other hand, no special care was taken to supress the electrode poralization for the measurement equipment used by Latikka *et al* (2001). Hence, the observed differences were clearly in the range of the measurement uncertainty, and the difference in the treatments of electrode poralization is assumed as the main cause.

Figures 4(a) and (b) compare dielectric properties of grey and white matter, respectively, in the frequency range from 10 MHz to 100 GHz. The plots in the figure 4 are from the original data or derived from reported empirical equations, while for a few cases, plots were reproduced from figures in the original reference using *Engauge Digitizer ver. 12.1*. Most of the data shown in the figures were obtained by *in vitro* measurements (except those for grey matter reported by Schmid *et al* (2003a) and Peyman *et al* (2007)). On the basis of the data reported by Gabriel *et al* (1996c), which are the most used data, the variabilities of the data were within approximately 30% for both conductivity and permittivity, except for the data reported by Bao *et al* (1997) and Mohammed *et al* (2016). These variabilities are larger than the difference between data from *in vivo* measurements and those reported by Gabriel *et al* (1996c). One of the possible reasons for the discrepancies between the data of Gabriel *et al* (1996c) and Mohammed *et al* (2016) is the different tissue temperatures. Better agreement with the data of Gabriel *et al* (1996c) can be observed upon adjusting the grey matter conductivity data reported by Mohammed *et al* (2016) for the temperature using the temperature coefficients for porcine brain obtained by Schmid *et al* (2003a) (see appendix B). Comparison of the data for grey matter obtained by Gabriel *et al* (1996c) at 37 °C and the corresponding temperature adjusted data reported by Schmid *et al* (2003b) revealed that the latter shows 10%–25% higher values. This discrepancy is most likely due to the fact that in Schmid *et al* (2003b), the measurement probe was placed on the grey matter while keeping the arachnoid intact, whereas the probe was placed on the grey matter after removing the arachnoid in Gabriel *et al* (1996c).

3.4. Review of muscle anisotropy

The anisotropy of the dielectric properties of muscle is observed in intermediate- and low-frequency bands, knowledge of which is essential for the precise electromagnetic modeling of human in these frequency bands. Summaries of the 5 papers presenting dielectric measurements of muscle anisotropy listed in table 4 are provided below.

Gabriel *et al* (1996b) reported the variation in the dielectric properties of ovine muscle *in vitro* measured along (parallel direction) and across (transverse direction) muscle fibers from 10 Hz to 20 GHz using coaxial probes. R Relevant differences in permittivity were observed up to 10 MHz, and the ratio of the permittivities measured along the parallel and transverse directions ranged from 2.4 (at several tens of Hz) to 0.2 (at several hundreds of kHz). Significant anisotropy in the conductivity was found below 1 MHz; the maximum to minimum ratio due to anisotopy was up to 1.5. The authors commented that the result may not represent the maximum variation (anisotropic factor) of the dielectric properties of muscle because of the nature of the polarization direction of the electric field induced by the coaxial probe.

Table 5. Overview of review results for other tissues in section 3.5.

Author	Frequency	Tissues	Source	State	Tissue temperature
Gabriel et al (1996b, 1996c)	10 Hz–20 GHz (in maximum)	13 tissues (heart, kidney, liver, lung, spleen, muscle, uterus, thyroid, testis, ovary, bladder, cartilage, and cortical bone)	Ovine, human, porcine	In vitro	37 °C
		Tongue	Human	In vivo	Not reported
Lu et al (1996)	100 kHz–500 MHz	7 fetal tissues (skin, muscle, heart, liver, kidney, spleen, and brain)	Human	In vitro	24 °C
El-Lakkani (2001)	20 Hz–100 kHz	Kidney and skeletal muscle	Murine	In vitro	37 °C
Akhtari et al (2002)	10–90 Hz	Bone (skull)	Human	In vitro	Not reported
Tang et al (2008)	1 Hz–4 MHz	Bone (skull)	Human	In vitro	36.5 °C
Haemmerich et al (2009)	10 Hz–1 MHz	Liver	Human	In vitro	Not reported
Gabriel et al (2009)	40 Hz–1 MHz	6 tissues (muscle, heart, skull, fat, lung, and liver)	Porcine	In vivo	Not reported
		4 body fluids (blood, bile, cerebrospinal fluid, and urine)		In vitro	37 °C
Abdalla et al (2010)	10 kHz–5 MHz	Blood	Human	In vitro	Not reported
Wilmink et al (2011)	0.13–1.6 THz	Muscle	Porcine	In vitro	Not reported
Peyman et al (2011)	0.2–10 GHz	Placenta, umbilical cord, and amniotic fluid	Human	In vitro	37 °C
Peyman and Gabriel (2012a)	40 MHz–20 GHz	Embryo and fetus	Rat	In vitro	37 °C
Peyman and Gabriel (2012b)	40 MHz–20 GHz	5 glandular tissues, ovary, and testis	Porcine	In vivo	37 °C
		5 body fluids		In vitro	
Sasaki et al (2013)	20–110 GHz	Blood	Porcine	In vitro	25 °C
Abdilla et al (2013)	0.5–40 GHz	Muscle and liver	Bovine and porcine	In vitro	37 °C
Sasaki et al (2015)	0.5–110 GHz	6 ocular tissues	Rabbit	In vitro	35 °C
		Aqueous humour	Porcine		
Fornes-Leal et al (2016)	0.5–18 GHz	Colon	Human	In vitro	Not reported
Li et al (2016)	50–500 MHz	Large intestine	Human	In vitro	24.9 °C–29.7 °C
Mohammed et al (2016)	0.3–3 GHz	Skull	Canine	In vitro	Not reported
Sasaki et al (2017)	1–100 GHz	Muscle	Porcine	In vitro	35 °C
Cheng and Fu (2018b)	0.5–8 GHz	Thyroid	Human	In vitro	Not reported
Gavazzi et al (2018)	0.2–10 GHz	Thyroid	Human	In vitro	19.1 ± 1.3 °C
Yu et al (2020)	1 MHz–4 GHz	Lymph node	Human	In vitro	24 °C
Mizuno et al (2021)	1 GHz–3 THz	Cornea	Porcine and rabbit	In vitro	35 °C
Putzeys et al (2021)	0.1 Hz–10 MHz	Perilymph	Human	In vitro	37 °C

Gabriel *et al* (2009) investigated the anisotropy of conductivities below 1 MHz by *in vivo* measurement of porcine skeletal muscle using a four-electrode method. Although several earlier studies reported more than a ten-fold variation in the conductivity of muscle tissue due to anisotropy, the maximum to minimum ratio due to anisotropy observed by Gabriel *et al* (2009) ranged from 1.2 to 1.9, i.e. slightly higher than that in their earlier study (Gabriel *et al* 1996b). They noted that the lack of correspondance between the data from different studies may due to differences in the probe geometry and the tissue structure.

Ahad *et al* (2009) measured rat skeletal muscle *in vitro* at 36 °C–37 °C using from 2 kHz to 1 MHz using a four-electrode method. The maximum to minimum ratio due to anisotropy ranged from 1.3 to 3.6 for the conductivity, while little anisotropy was observed for the permittivity, which was comparable to twice the standard error of the mean.

Sanchez *et al* (2014) measured the anisotropy of rat muscles *in vitro* at 37 °C using a four-electrode method. The resistivities of soleus and gastrocnemius muscles were measured at frequencies from 1 kHz to 10 MHz. They also reported parametric models for the complex resistivity of each muscle tissue in the longitudinal and transverse directions to the muscle fibers. The maximum to minimum ratios due to anisotropy were up to 5.6 and 3.0 for the soleus and gastrocnemius muscles, respectively.

Kwon *et al* (2019) reported the anisotropy of skeletal muscle at 30 kHz–1 MHz on the basis of impedance measurement using a multipole needle (four-electrode technique). Skeletal muscles of three ovine samples were measured *in vitro* at room temperature (25 °C). Their results demonstrated little variation of the measurement data due to anisotropy, i.e. the maximum to minimum ratio due to anisotropy was within 1.2 in the considered frequency range.

3.5. Review of other tissues

Summaries of the 24 papers presenting dielectric measurements of tissues other than skin, adipose, and brain tissues listed in table 5 are provided below.

Gabriel *et al* (1996b) measured the dielectric properties of 17 tissues (including those of skin, adipose, brain, and muscle tissues summarized in sections 3.1–3.4) at body temperature using three coaxial probes. Measurements were conducted using ovine tissues in general and some porcine tissues *in vitro*. Seven tissues out of these 17 were obtained from human autopsy samples, and human tongue and skin (see section 3.1) were measured *in vivo*. Ten of the 17 tissues were measured at frequencies from 10 Hz to 20 GHz, and the other tissues were measured at frequencies from around 1 MHz to 20 GHz. On the basis of their measurement and their review (Gabriel *et al* 1996a), parametric models were developed using four-pole Cole–Cole models (Gabriel *et al* 1996c).

Lu *et al* (1996) reported the dielectric properties of human fetal tissues *in vitro*. The fetal gestation periods were estimated as 14–16 weeks. The dielectric properties of skin, muscle, heart, liver, kidney, spleen, and brain at 24 °C at frequencies from 100 kHz to 500 MHz were reported. They found that, in general, the dielectric properties of human fetal tissues were comparable to those of human and mammary tissues reported by Stuchly and Stuchly (1980b) and Foster and Schwan (1989), although some discrepancies were observed for the conductivity at low frequencies for lung, liver, and brain tissues.

El-Lakkani (2001) measured the dielectric properties of murine tissues, i.e. kidney and skeletal muscle, *in vitro* from 20 Hz to 100 kHz at 37 °C using RLC bridges. Two different parametric models were compared and it was found that a two-pole Cole–Cole model showed better agreement with their measurement results.

Akhtari *et al* (2002) measured the conductivities of human bone (skull) *in vitro* at room temperature from 10 to 90 Hz using four-electrode method. Human bone obtained from four patients by intracranial surgery were measured at different locations, i.e. compact, spongiosum, and bulk layers. They found that the conductivity values for bone were frequency dependent in the considered frequency range and they were significantly different for the spongiform, the top compact, and lower compact layers.

Tang *et al* (2008) measured the resistivity of human bone (skull) *in vitro* from 1 Hz to 4 MHz at 36.5 °C using a four-electrode method. A total of 48 skull flaps from 48 patients (20–74 years of age) were excised by intracranial surgery, mainly from the frontal–temporal–parietal region (46 samples). It was found that an increase in the component percentages of the skull dipole (i.e. the spongious region between the compact bone layers) affect the decrease in the resistivity. In a later work by the same group (Tang *et al* 2009), parametric models of six types of skull samples based on their measurements were presented.

Haemmerich *et al* (2009) measured the conductivity of human liver *in vitro* from 10 Hz to 1 MHz using a four-electrode method. Normal tissues were separated from tumors of six patients by surgical removal. The measured conductivities of normal liver tissues were up to 25%–45% lower than those reported by Gabriel *et al* (1996b). The reason for the observed discrepancy was suggested to be the different post-excision times of the samples during the measurements (30–60 min in Haemmerich *et al* (2009) and 24−48 h in Gabriel *et al* (1996b)).

Gabriel *et al* (2009) reported the conductivities of porcine tissues from 40 Hz to 1 MHz as a supplement of their database (Gabriel *et al* 1996b, 1996c). The dielectric conductivities of five tissues, i.e. muscle, heart, liver, lung, and bone (skull), were measured *in vivo* and those of three body fluids, i.e. urine, bile, and blood, were measured *in vitro* at approximately 37 °C using a four-electrode method.

Abdalla *et al* (2010) measured the dielectric properties of blood from 20 normal and diabetic human patients *in vitro* at room temperature from 10 kHz to 5 MHz using a parallel plate method. Blood samples were obtained from 20 patients. An empirical relating between the conductivity and a mechanical parameter (viscosity) of the blood was presented.

Wilmink *et al* (2011) measured the optical properties, i.e. refractive index and absorption coefficient, of porcine muscle *in vitro* from 0.13 to 1.6 THz at room temperature using THz-TDS. Measured results were compared with those measured by other groups.

Peyman *et al* (2011) measured the dielectric properties of human tissues, i.e. placenta, umbilical cord, and amniotic fluid, *in vitro* from 0.2 to 10 GHz using a coaxial probe. They found that the dielectric properties of the umbilical cord were higher than those of the placenta due to a higher water content in the umbilical cord. The results also demonstrate significant differences in the dielectric properties of amniotic and cerebrospinal fluids. In addition, parametric models of tissue dielectric properties were reported.

Peyman and Gabriel (2012a) measured the dielectric properties of rat embryo and fetus from 40 MHz to 20 GHz at 37 °C using a coaxial probe. An embryo or fetus was homogenized at each stage from 18 to 20 d of gestation. They observed a slight decrease in dielectric properties with increased gestation, although the differences were within one standard deviation in each measurement, i.e. around 5% for most cases.

Peyman and Gabriel (2012b) measured the dielectric properties of porcine glandular tissues, gonads, and body fluids from 50 MHz to 20 GHz using a coaxial probe. The glandular tissues (adrenal gland, mesenteric lymph node, salivary glands, thymus, and thyroid glands) and gonads (ovaries and testis) were measured *in vivo*, and the body fluids (aqueous humor, vitreous humor, bile, blood, and urine) were measured *in vitro* at 37 °C. Parametric models based on their measurement results were also reported.

Sasaki *et al* (2013) measured the dielectric properties of porcine blood from 20 to 110 GHz at 25 °C using free-space method. Measured results were compared with the values reported by Alison and Sheppard (1993) and the maximum differences in the dielectric properties were around 20%.

Abdilla *et al* (2013) measured the dielectric properties of muscle and liver *in vitro* excised from bovine and porcine at frequencies from 0.5 to 40 GHz at 37 °C using a coaxial probe. Parametric models using a single-pole Cole–Cole model were also reported.

Sasaki *et al* (2015) measured the dielectric properties of ocular tissues, i.e. cornea, aqueous humor, vitreous humor, sclera, and iris, *in vitro* at 35 °C from 0.5 to 110 GHz using a coaxial probe. With the exception of the porcine aqueous humor, all ocular tissues were obtained from rabbits. They found that the dielectric properties of the aqueous humor were almost the same as those of pure water at frequencies above 13 GHz.

Fornes-Leal *et al* (2016) measured the dielectric properties of human colon *in vitro* from 0.5 to 18 GHz using a coaxial probe. Tissues of healthy and malignant colon were obtained from 20 patients by surgery. Parametric models using a two-pole Cole–Cole model were also reported. The dielectric properties of healthy colon were slightly lower than those reported by Gabriel *et al* (1996c).

Li *et al* (2016) measured tissues from human large intestines, i.e. colon and rectum, at 24.9 °C–29.7 °C from 50 to 500 MHz using a coaxial probe. Normal and malignant tissues were collected by cancer surgery of 85 patients (23–83 years of age). Parametric models using a single-pole Cole–Cole model were also reported. Differences in the measured dielectric properties for normal human colon from those for ovine tissue obtained by Gabriel (1996) were within 20%.

Mohammed *et al* (2016) measured the dielectric properties of canine skull in addition to canine brain tissues (see section 3.3.1) *in vitro* at room temperature from 0.3 to 3 GHz using a coaxial probe. The effect of aging on the dielectric properties was also investigated and discussed (details are given in section 5.3).

Sasaki *et al* (2017) measured the dielectric properties of porcine muscle *in vitro* at 35 °C from 1 to 100 GHz using a coaxial probe, and the obtained data were used for the assessment of human exposure to electromagnetic waves.

Cheng and Fu (2018b) measured the dielectric properties of human thyroid tissues *in vitro* from 0.5 to 8 GHz using a coaxial probe. Tissues of normal and cancerous thyroid were obtained from 48 patients by thyroidectomy.

Gavazzi *et al* (2018) measured the dielectric properties of human thyroid tissues *in vitro* at 19.1 ± 0.3 °C from 0.2 to 10 GHz using a coaxial probe. Tissues were collected from 14 patients (19–80 years of age) by surgery and histologically classified into five types including normal (healthy) and malignant tissues. Parametric models using a two-pole Cole–Cole model were also reported.

Yu *et al* (2020) measured the dielectric properties of human (intrathoracic) lymph nodes *in vitro*, measured at approximately 24 ± 2.4 °C from 1 MHz to 4 GHz using a coaxial probe. Normal and metastatic lymph node

samples were obtained by cancer surgery of 76 patients (30–78 years of age). Parametric models using a two-pole Cole–Cole model were also reported. The measured dielectric properties of the lymph nodes were lower than those repoted by Peyman and Gabriel (2012b), who measured porcine mesenteric lymph nodes *in vivo* at 37 °C, and the difference was attributed to differences in the measurement procedure.

Mizuno *et al* (2021) measured the dielectric properties of cornea *in vitro* at approximately 35 °C from 1 GHz to 3 THz using a coaxial sensor (1–100 GHz) and THz-TDS (0.1–3 THz). The properties of rabbit and porcine cornea were compared. They commented that the difference in the dielectric characteristics was mainly caused by differences in the water content, which is the dominant factor causing individual deviations.

Putzeys *et al* (2021) measured the dielectric properties of human perilymph *in vitro* at 37 °C from 0.1 Hz to 10 MHz using a two-electrode method. The time dependence of the dielectric properties within 48 h after excision was also investigated at a maintained temperature, and no significant change was observed up to 11 h after excision. Moreover, they found a clear difference between data obtained from previously frozen and fresh samples.

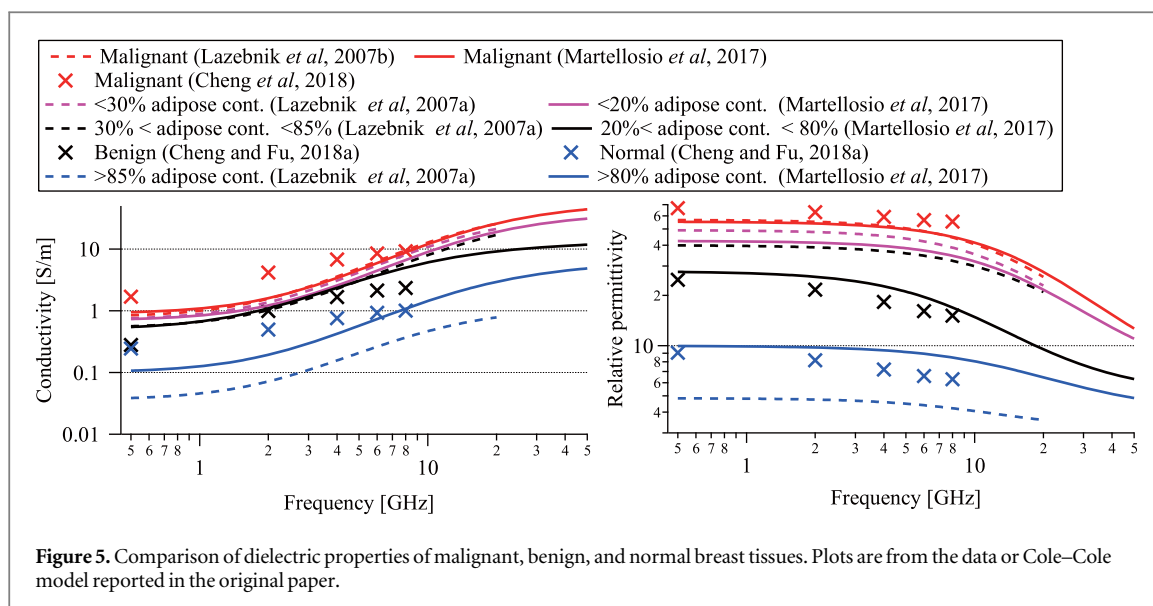### 3.6. Discussion and research needed

Data for the dielectric properties of skin have been obtained in numerous studies, with a clear focus on the frequency range of above 500 MHz. Taking into account the biological variation of skin and the different measurement conditions applied in different studies, the reported results are in reasonable agreement above 500 MHz. In contrast, data for skin conductivity and permittivity are scarce at frequencies below 500 MHz, and the little available data show significant spread. This is most likely caused by the complex layered structure of the skin (i.e. several layers of varying thickness and significantly different dielectric properties) and uncertainties in the measurement technique (e.g. electrode polarization). Nevertheless, the dielectric properties of skin in the low-frequency region play an important role in the assessments of human exposure as well as in medical applications. Therefore, accurate determination of the dielectric properties of the different skin tissue layers, such as the stratum corneum, epidermis and dermis, particularly in the frequency range below 10 kHz, is seen as an essential research need. Similarly, care should be taken to account for the detailed structure of skin at the frequencies of the millimeter-wave and sub-millimeter-wave bands because of the short wavelengths and because the complex structure of skin may exhibit characteristic electromagnetic responses (e.g. Feldman *et al* (2009), Tripathi *et al* (2018)).

For adipose tissues, the data obtained from the literature showed a large variation dependent on the adipose or water content, as discussed in section 3.2.2, with a maximum to minimum ratio of up to around 30 observed for conductivity. Lazebnik *et al* (2007a, 2007b) and Martellosio *et al* (2017) demonstrated a correlation between the dielectric properties of breast tissue and the adipose content. Because the fat content of adipose tissue varies from 40% to 80% with age (ICRP 2002), it may be useful to determine the correlation between the dielectric properties and the fat/water contents of adipose tissue. If the relationship between the distribution of the fat/water content in adipose tissue and the dielectric properties can be clarified, further advances in the electromagnetic modeling of the human body can be expected.

For brain tissues, there were only minor discrepancies in dielectric properties of up to 10% between those reported by different groups (see figure 4), and the frequency trends were consistent with each other from 50 MHz to around 20 GHz. There is a lack of knowledge of dielectric properties of brain tissues at frequencies over 20 GHz. However, exposure levels of brain tissues are less dominant than those of surface tissues from the human protection for exposure to millimeter and sub-millimeter waves point of view, and to date no medical applications employing this frequency range exist. Because of the lack of needs for dielectric data of brain tissues at frequencies over 20 GHz, the dielectric measurements of brain tissues would not be highly necessary at this moment. In contrast, obtaining accurate data for brain tissues below 50 MHz with clarification of the measurement uncertainty should be considered a priority.

Some groups have investigated the anisotropy of muscle tissue, and the reported results show significant discrepancies. The main reason is that, owing to the methodological limitations concerning the measurement cell/probe, it is difficult to accurately match the electric field vector with the direction of the muscle fiber. Therefore, the accurate determination of tissue anisotropy (not necessarily only for muscle tissue) is also considered an important issue in future research along with the improvement of measurement accuracy.

The empirical equations derived by Gabriel *et al* (1996c) and Gabriel and Gabriel (1997) have been widely used in the electromagnetic modeling of the human body. Although agreement between measured data and values derived from the empirical equations is desirable, variations have been found (e.g. Schmid *et al* (2013), Sasaki *et al* (2014b)). The variations depend on the tissue and frequency, while mean variations of approximately 10% in the frequency range from 1 MHz to 20 GHz have been reported for most tissues (Sasaki *et al* 2014b). Although the empirical equations were developed on the basis of measurements up to 20 GHz (Gabriel *et al* 1996b, Gabriel and Gabriel 1997), data for frequencies above 20 GHz extrapolated from the empirical equations
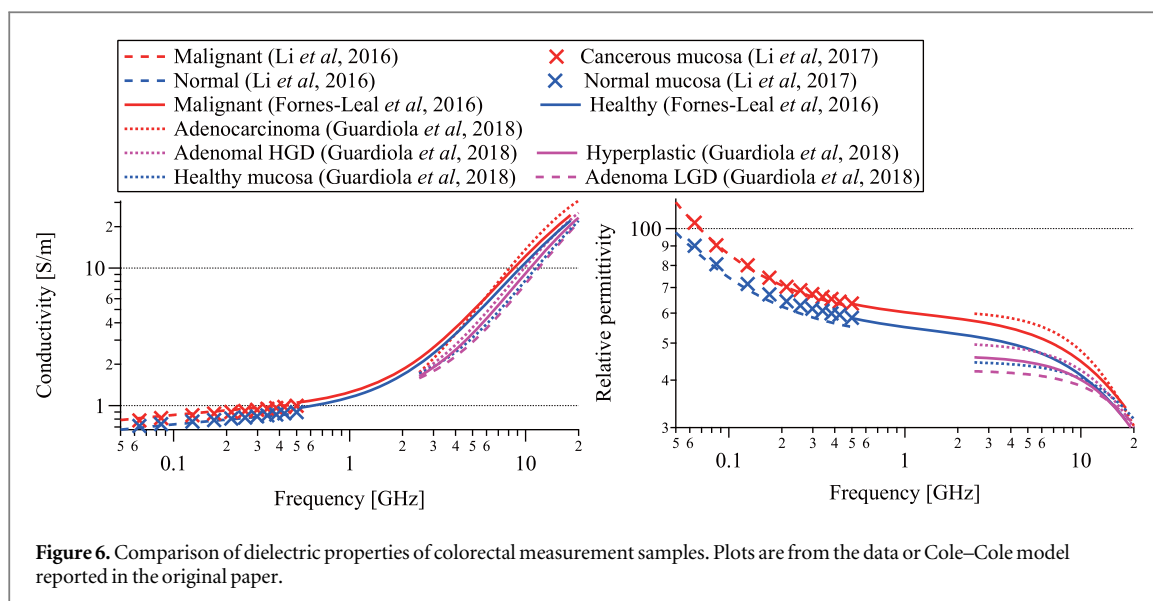
Figure 5. Comparison of dielectric properties of malignant, benign, and normal breast tissues. Plots are from the data or Cole–Cole model reported in the original paper.

Table 6. Overview of review results for malignant breast tissues.

Author	Frequency	Malignancy type	Notes
Ahmed *et al* (2006)	1 kHz–100 kHz	Infiltrating breast carcinoma	15 specimens: 5 invasive ductal carcinomas without lymph node metastasis, 5 invasive ductal carcinomas with lymph node metastasis, and 5 invasive lobular carcinomas without lymph node metastasis; 25 °C
Lazebnik *et al* (2007b)	0.5–20 GHz	Benign and malignant breast tissues	196 patients, 319 specimens; 18 °C–27.2 °C.
Sugitani *et al* (2014)	0.5–20 GHz	Tumor tissues	35 patients, 102 specimens; 18 °C–24.1 °C.
Martellosio *et al* (2017)	0.5–50 GHz	Malignant tissues	53 patients, 222 specimens (166 normal, 56 tumor samples); 19 °C–22 °C
Cheng and Fu (2018a)	0.5–8 GHz	Benign and malignant breast tissues	98 patients, 509 specimens; temperature not reported
Shawki *et al* (2022)	50 Hz–100 kHz	Malignant tissues	15 patients, 15 samples; temperature not reported

have been adopted in computational dosimetry (e.g. Hashimoto *et al* (2017), Laakso *et al* 2017, Li *et al* (2021)). Comparing the extrapolated data for each skin (Gabriel *et al* 1996b), which are of general interest for millimeter-wave and sub-millimeter-wave frequencies, with the data reported in this review, we found that the extrapolated results for skin, particularly for wet skin, show good agreement with data for the dermis reported by Sasaki *et al* (2014a, 2017) up to a frequency of 300 GHz (see table C1). For adipose tissue, the extrapolated results for blood-infiltrated fat were at the lower end of the dielectric properties reported for frequencies up to 300 GHz, and the conductivity at 1 THz obtained by extrapolation was half the value obtained by Ashworth *et al* (2009) (see table C2). Although these observations partly demonstrate the applicability of the extrapolated results, they also suggest the importance of obtaining the properties of real tissues to justify the result of electromagnetic modeling of the human body.

Many dielectric measurements of tissues in the radiofrequency domain, i.e. 100 MHz to 20 GHz, have been reported, but data on dielectric properties below 100 MHz and above 20 GHz are scarce. In the low-frequency region, a large uncertainty in the dielectric measurement is expected compared with the high-frequency region due to the electrode polarization effect. Therefore, there are large discrepancies between measurements and, in particular, intercomparison becomes difficult below 1 MHz. There has been little detailed research on the measurement uncertainty at frequencies below 100 MHz and over 100 GHz, in contrast to the frequency range between these values (see, for example, Gabriel and Peyman (2006)). Quantification of the dominant factors of measurement uncertainty will be essential for obtaining accurate data, and it may be possible to distinguish the factors peculiar to tissues, such as the effects of physiological conditions.

Figure 6. Comparison of dielectric properties of colorectal measurement samples. Plots are from the data or Cole–Cole model reported in the original paper.

4. Dielectric characterization of malignant tissues

A systematic search of the literature reporting the dielectric measurements of human malignant tissues was conducted (August 2021) using three search engines: Web of Science, PubMed, and Google Scholar; details of the search terms are given in appendix A. In total, 25 works presenting measurements from 10 organ/tissue types were found. For breast and colon, which have been the most studied organs to date, review results are respectively summarized in sections 4.1 and 4.2, which include comparisons between reported data. Review results for the other organs/tissues are summarized in section 4.3. The organ/tissue types include urine, blood, saliva, colon, liver, lymph nodes, prostate, skin, and thyroid. Section 4.4 provides a discussion of the primary findings with an emphasis on the limitations and gaps in the data available, which highlight the need for more research in this area.

4.1. Review of breast tissue

Summaries of the six papers presenting dielectric measurements of malignant breast tissues listed in table 6 are provided below.

Ahmed (2006) conducted low-frequency dielectric measurements (1–100 kHz) on normal and breast carcinoma specimens at 25 °C using a two-electrode method. The dielectric properties were fitted using a single-pole Cole–Cole model, with only the relaxation time reported. It resulted that tumor tissues had an average dielectric relaxation time of between 3 and 5 μs and that the normalized conductivity and permittivity of tumor tissues were significantly higher than the surrounding tissues. Additionally, both tumor tissues and the surrounding tissues covered a broad distribution of relaxation times, which was attributed to different degrees of tumor cell infiltration.

Lazebnik *et al* (2007b) reported on the dielectric properties of normal (adipose, glandular and fibroconnective), malignant (invasive and non-invasive ductal and lobular carcinomas, IDC, DCIS, ILC and LCIS) and benign (fibroadenomas and cysts) breast tissue samples obtained from cancer surgery. Dielectric measurements were conducted from 0.5 to 20 GHz using a coaxial probe on 319 samples excised from 196 patients undergoing cancer surgery. In this study, the effects of temperature, time between excision and measurement, and patient age were analyzed at different frequencies. Note that details of the effect of the time between excision and measurement and the aging effect are given in sections 5.1 and 5.3, respectively. They found that the dielectric properties of malignant tissues are high and span a relatively small range compared with those of benign and other normal breast tissues with similar adipose content. The Cole–Cole parameters of the curves corresponding to the 50th percentile for cancer samples containing 30% or greater malignant tissue content were published along with three categories of tissues with different adipose contents, and the data are illustrated in figure 5.

In Sugitani *et al* (2014), the dielectric properties of *in vitro* breast tumor tissues from 0.5 to 20 GHz were characterized at room temperature (18 °C–24.1 °C) using a coaxial probe. The variability of the complex permittivity of the tumor tissues was also investigated, with the significant variability attributed to the volume fraction of cancer cells in the measured volume.

Table 7. Overview of review results for colorectal cancer tissues.

Author	Frequency	Malignancy type	Notes
Fornes-Leal *et al* (2016)	0.5–18 GHz	Colorectal cancer	20 patients; temperature not reported
Li *et al* (2016)	50–500 MHz		85 patients; 24.9 °C–29.7 °C
Li *et al* (2017)	50–500 MHz		130 patients; mean 26.6 °C–27.3 °C
Guardiola *et al* (2018)	0.5–20 GHz		23 patients; 20 °C–22 °C

A similar method of tissue classification by Lazebnik *et al* (2007b) was used by Martellosio *et al* (2017), who also used a coaxial probe to conduct measurements on excised human breast tumor tissues from 0.5 to 50 GHz. The tissue groups were also based on adipose content, namely, tissues with adipose contents of less than 20%, more than 80%, and between 20% and 80%. The dielectric characterization of both normal and tumor breast tissues obtained from 222 tissues (166 normal samples, 56 tumor samples) from 53 patients was performed. Tumor tissues were classified as invasive and non-invasive, and they found that the mean value obtained for tumor tissues is higher than that of normal breast tissues. The effect of time between excision and measurement and patient age were also investigated, which summary are shown in sections 5.1 and 5.3, respectively. The measured data were fitted using a single-pole Cole–Cole model for both normal and malignant human breast tissues, and the data are illustrated in figure 5.

In Cheng and Fu (2018a), the dielectric properties of benign and malignant breast tissues were characterized in the frequency range of 0.5–8 GHz using a coaxial probe. A total of 508 samples obtained from 98 patients undergoing surgery were considered, and excised specimens were stored in heated, sealed, and insulated containers to minimized desiccation. However, no sample temperatures were recorded. The relative permittivity and conductivity at 0.5, 2, 4, 6 and 8 GHz were reported for benign and cancer tissues, as shown in figure 5.

Shawki *et al* (2022) investigated the dielectric properties of normal and malignant tissues at low frequencies (50 Hz–100 kHz), using a cylindrical cell connected to an LCR meter. Measurements were conducted on 15 samples obtained from 15 patients and the calculated average relative permittivity for the normal tissues varied between 1.79×10^{13} at 50 Hz and 1430 at 100 kHz. Higher values of between 7.32×10^{15} at 50 Hz and 21800 at 100 kHz were obtained for the malignant tissues. The calculated average conductivity for the normal and malignant tissues ranged between 13.3 (50 Hz) and 3.15 (100 kHz) and between 1330 and 189 mS m^{-1}, respectively. Additionally, the relative permittivity and conductivity of the malignant breast tissues were higher than those of the surrounding normal tissues, in agreement with all other studies on breast tissues.

4.2. Review of colon tissue

Summaries of four papers presenting dielectric measurements of colorectal cancer tissues listed in table 7 are provided below.

In Fornes-Leal *et al* (2016), healthy and malignant colon tissues were measured *in vitro* from 0.5 to 18 GHz using a coaxial probe. The resulting mean relative permittivity and conductivity were fitted to a two-pole Cole–Cole model as illustrated in figure 6. It was found that the relative permittivity is statistically significantly higher for cancerous colon tissues than for healthy tissues, with an average difference of 8.8% across the whole frequency range. For conductivity, the average difference between cancerous and healthy tissues across the frequency range was found to be 10.6%, but this difference was not statistically significant owing to the increased standard deviation of the measurements.

In Li *et al* (2016), the dielectric properties of excised malignant colorectal samples were measured using a coaxial probe in the Larmor frequency range (50–500 MHz) at tissue temperatures of 24.9 °C–29.7 °C. The median dielectric properties of the normal and malignant tissues (from the Cole–Cole model) are plotted in figure 6 across the frequency range. Statistically significant differences were found between the permittivity and conductivity of the normal and malignant tissues for each representative frequency point (64, 128, 170, 298, 400, and 468 MHz). At 128 MHz, for example, the median permittivity of normal samples was 69.2, compared with a value of 79.3 (14.6% higher) for malignant samples, and the median conductivity of normal samples was 0.753 S m^{-1}, whereas that for malignant samples was 0.881 S m^{-1} (17% higher).

In a later work by the same group (Li *et al* 2017), freshly excised colorectal cancerous samples were measured from 50 to 500 MHz using a coaxial probe to examine the dielectric properties across tumor stages ($\leqslant$I, II, III, and IV). The dielectric properties of normal mucosa (26.6 $\pm$ 2.4 °C), cancerous mucosa (26.9 $\pm$ 2.6 °C), and cancerous serosa (27.3 $\pm$ 2.5 °C) were measured. The mean dielectric properties of the normal mucosa and cancerous mucosa are plotted in figure 6 across the frequency range. They found that both the relative permittivity and conductivity were found to be statistically significantly greater for cancerous mucosa than for normal mucosa. Furthermore, the dielectric properties were found to increase with the tumor stage in general.

Table 8. Overview of review results for other tissue/organ types.

Author	Frequency	Tissue	Malignancy type	Notes
Ghanbarzadeh-Daghian *et al* (2020)	120 Hz	Blood	Hematologic cancer	12 pediatric cancer patients; temperature not reported
Ibrahim *et al* (2008)	20 Hz–100 kHz	Blood (liver)	DNA in blood from hepatocellular carcinoma patients	10 patients with hepatocellular carcinoma; 20 °C
Batyuk *et al* (2018)	9.2 GHz	Blood (breast and lung)	Suspension of red blood cells (RBCs) and RBC ghosts from breast and lung cancer patients	62 patients with breast and lung cancer; 1 °C–46 °C
O'Rourke *et al* (2007)	0.5–20 GHz	Liver	Malignant liver tissue: hepatocellular cancer (HCC) and hepatic metastases	*In vitro* (20 °C–24 °C) and *in vivo*; 6 patients (4 livers *in vitro*; 5 livers *in vivo*)
Wang *et al* (2014)	10 Hz–100 MHz	Liver	Hepatocellular carcinoma, hepatic fibrosis, and liver hemangioma	132 samples from 116 patients with average age 49 ± 12 years; 26 normal liver samples, 31 HCC, 28 liver hemangioma and 47 hepatic fibrosis
Peyman *et al* (2015)	100 MHz–5 GHz	Liver	Hemangioma, hepatocellular carcinoma, metastasis of adenocarcinoma of stomach, and colon and tumor contained in intracellular space	6 patients; 25 ± 0.5 °C
Halter *et al* (2009)	0.1–100 kHz	Prostate	Prostate adenocarcinomas	50 *in vitro* human prostates; 20 °C
Yu *et al* (2020)	1 MHz–4 GHz	Intrathoracic lymph node	Metastatic and non-metastatic lymph nodes	41 lung cancer metastatic thoracic lymph nodes and 178 non-metastatic lung thoracic lymph nodes from 74 patients; 24 ± 2.4 °C
Ranade *et al* (2016)	10 MHz–20 GHz	Saliva	Oral cancer	48 patients with oral cancer (squamous cell carcinoma)
Mayrovitz *et al* (2018)	300 MHz	Skin	Skin basal cell carcinoma (BCC)	32 patients with BCC; 21.6 ± 1.2 °C
Mirbeik-Sabzevari *et al* (2018)	0.5–50 GHz	Skin	Malignant skin tissues	41 patients with basal cell carcinoma or squamous cell carcinoma; 22 °C
Ibrahim *et al* (2012)	0.1–10 MHz	Urine	Urine DNA of bladder cancer patients	45 patients with bladder cancer (30 urothelial cell carcinoma, 15 squamous cell carcinoma); 20 ± 0.1 °C
Cheng and Fu (2018b)	0.5–8 GHz	Thyroid	Normal and papillary thyroid cancer	48 patients (normal, malignant); temperature not reported
Gavazzi *et al* (2018)	0.2–20 GHz	Thyroid	Normal, diseased, and malignant thyroid tissues (Normal, struma, thyroiditis, adenoma, and cancer)	14 patients; data fitted to Cole–Cole model; 19.1 ± 1.3 °C
Huang *et al* (2021)	1–4000 MHz	Thyroid	Benign and malignant thyroid nodules (nodular goiter, follicular adenoma, papillary carcinoma, and follicular carcinoma)	155 patients; 25 °C

In Guardiola *et al* (2018), freshly excised colon samples (20 °C–22 °C) were measured using a coaxial probe (0.5–20 GHz). The median measured complex permittivity for each group of colon tissues (healthy mucosa, hyperplastic polyps, adenomas with low-grade dysplasia (LGD), adenomas with high-grade dysplasia (HGD), and adenocarcinoma) from 2.5 to 20 GHz (the reported frequency range for the Debye model parameters) is shown in figure 6. It was found that the complex permittivity is correlated with the dysplasia grade of polyps, with higher measured relative permittivity and conductivity more likely to be associated with cancerous tissues. High average differences were found between cancerous and benign tissues, e.g. 20%–30% difference in relative permittivity between 2 and 8 GHz and 30%–60% difference in conductivity between 5 and 8 GHz. Cancerous tissues were able to be distinguished from non-cancerous tissues with a sensitivity of 100% and a specificity of 95%.

4.3. Review of other organ/tissue types

Summaries of the 15 papers presenting dielectric measurements of malignant tissues other than breast and colon tissues listed in table 8 are provided below.

4.3.1. Blood-related cancers

Ghanbarzadeh-Daghian *et al* (2020) measured blood samples from 12 pediatric patients with different types of hematologic cancers at 120 Hz at room temperature using an LCR meter. The relative permittivity ranged from 10.3×10^6 to 16.4×10^6 for patients with cancer and from 5.1×10^6 to 8.8×10^6 for healthy donors, indicating that samples from patients with cancer had approximately two times higher measured relative permittivities than those of healthy individuals.

4.3.2. Blood of individuals with other malignancies

In Ibrahim *et al* (2008), the dielectric properties of DNA from blood samples of patients with liver cancer were studied to examine the potential diagnostic ability of such measurements. Three groups were studied: (i) patients with hepatocellular carcinoma (HCC); (ii) patients with chronic hepatitis C (HCV) and (iii) healthy patients as a control. Dielectric measurements were conducted on DNA diluted in sterilized water at 20 °C from 20 Hz to 100 kHz using a precision component analyzer with a conductivity cell. The results indicate that the conductivity of the DNA suspension from HCC patients (and those with chronic HCV) was significantly higher than that of healthy patients. Also, the relative permittivity of the DNA suspension from patients with HCC was significantly higher than that of both patients with HCV and the normal control group below about 100 Hz.

Aiming to investigate the potential for early diagnosis of cancer and monitoring of cancer treatment, Batyuk and Kizilova (2018) obtained the dielectric properties of suspensions of red blood cells (RBCs) and RBC ghosts from patients with breast and lung cancers at 9.2 GHz in the temperature range of 1 °C–46 °C by resonance-based dielectrometry measurement. For the RBCs from cancer patients, the relative permittivity varied from approximately 40 to 60 over the temperature range, whereas for the RBC ghosts from cancer patients, the change was from approximately 40 to 70 over the same range. For the conductivity, a similar trend was observed for both RBCs and RBC ghosts. The relative permittivity was found to be higher in blood from cancer donors than in blood from healthy patients.

4.3.3. Liver

O'Rourke *et al* (2007) measured the dielectric properties of human normal, malignant, and cirrhotic liver tissue *in vivo* and *in vitro* from 0.5 to 20 GHz using a coaxial probe. In total, four livers *in vitro* and five livers *in vivo* were considered, where the temperature of the *in vitro* samples varied between 20 °C and 24 °C. The malignant liver tissue category consisted of one primary HCC tumor, five metastatic tumors, one pancreatic tumor, and three colorectal tumors. They reported that there was almost no statistically significant difference between *in vivo* normal and malignant tissues but a statistically significant difference between *in vitro* normal and malignant tissues at both 915 MHz and 2.45 GHz. The Cole–Cole parameters for each tissue type were also presented for their *in vitro* measurements.

Wang *et al* (2014) conducted *in vitro* measurements of liver tissues (normal, HCC, hepatic fibrosis, and liver hemangioma) from 10 Hz to 10 MHz using a four-electrode method. It was observed that liver with hemangioma had higher conductivity than the other tissues. Below 1 MHz, the conductivity of hepatic fibrosis tissues was the largest, followed by tissues from normal liver and HCC. The differences among the three tissues gradually decreased with increasing frequency. The changes in permittivity of the four types of liver tissues were similar, with the permittivity rapidly decreasing below 1 kHz. The measured data were also fitted to a two-pole Cole–Cole model, and it was found that the parameters of dispersion in the kHz frequency range can be used to distinguish between normal, HCC, hepatic fibrosis, and hemangioma tissues.

Peyman *et al* (2015) investigated the variation of dielectric properties due to pathological changes in human liver. Six patients were considered with the following pathological conditions: hemangioma, hepatocellular carcinoma, metastasis of adenocarcinoma of stomach, and colon and a tumour contained in intracellular space. Dielectric measurements were conducted at $25 \pm 0.5\,°C$ from 100 MHz to 5 GHz using a coaxial probe and Cole–Cole parameters were reported for each tumour type. For each patient, higher dielectric properties for tumour tissues were observed compared to normal tissue and this was attributed to the fact that tumour cells allow more for the accumulation of higher sodium and water contents than normal cells.

4.3.4. Prostate

In Halter *et al* (2009), a four-electrode probe was used to measure the conductivity and permittivity of 50 human prostates *in vitro* at 20 °C from 0.1 to 100 kHz. It was found that the conductivity of cancer tissues was below those of non-cancerous glandular and stromal tissues across all frequency points above 1 kHz. While, no significant differences were found between the conductivities of cancerous and benign tissues. The permittivity of cancer tissues, on the other hand, was significantly higher than that of all non-malignant tissues at 100 kHz.

4.3.5. Lymph nodes

Yu *et al* (2020) reported the dielectric properties of *in vitro* normal and metastatic intrathoracic lymph nodes. The measured data consisted of dielectric measurements on 41 metastatic lymph nodes and 178 non-metastatic lung thoracic lymph nodes obtained from 74 patients. Measurements were conducted on samples at $24 \pm 2.4\,°C$ from 50 MHz to 4 GHz using a coaxial probe. The results showed that the permittivity and conductivity of metastatic thoracic lymph nodes were higher than those of non-metastatic thoracic lymph nodes. The data were also fitted to a two-pole Cole–Cole model.

4.3.6. Saliva

In Ranade *et al* (2016), the dielectric properties of saliva samples from oral cancer patients were measured using time-domain reflectometry (10 MHz–20 GHz). The malignant samples had higher average values than the control group for both relaxation time and conductivity. No significant difference was observed for permittivity between the malignant and control groups, while statistically significant difference was observed between the average conductivity of the malignant and control groups. Within the malignant group, both average conductivity and permittivity increased from grade I to grade II and the relaxation time decreased, whereas the trends in all three measured parameters were inconsistent across stages I to IV.

4.3.7. Skin

Mayrovitz *et al* (2018) examined the potential for permittivity to be used to differentiate between skin cancer lesions and non-cancerous skin. *In vivo* measurements on basal cell carcinoma (BCC) and non-cancerous lesions were performed using a coaxial probe (at a room temperature of $21.6 \pm 1.2\,°C$). The relative permittivity was found to be 22.4 ± 16.2 for BCC lesions and 14.5 ± 9.0 for non-cancerous lesions. Much higher values of 38.1 ± 15.2 and 29.1 ± 9.0 were found for the contralateral (unaffected) skin in the BCC and non-cancerous groups, respectively. However, the permittivity values were not statistically different between BCC lesions and non-cancerous lesions.

In Mirbeik-Sabzevari *et al* (2018), skin tissue samples (BCC, squamous cell carcinoma (SCC), and normal) were measured at 22 °C from 0.5 to 50 GHz using a coaxial probe. Over the entire frequency band, malignant BCC samples had statistically significantly higher permittivity and conductivity than normal skin tissue. For the malignant SCC samples, statistically significant differences relative to the normal samples were also found across the frequency range, with a higher real part but lower imaginary part over the whole band. Maximum differences of 15 and 111% were found between the dielectric properties of normal and BCC samples and between those of normal and SCC samples, respectively.

4.3.8. Urine

In Ibrahim and Ghannam (2012), the dielectric properties of DNA suspensions from human urine samples were examined in the context of investigating such dielectric properties as a potential marker of bladder malignancy in cancer screening. Urine was collected from (i) patients with bladder diseases, (ii) patients with non-malignant (benign) urothelial diseases, and (iii) a control group. Using a loss factor meter, data were collected from 0.1 to 10 MHz (samples at $20 \pm 0.1\,°C$). The relative permittivity was found to decrease from approximately 2400 at 0.1 MHz to approximately 500 at 10 MHz, while the conductivity increased from close to zero to approximately $0.12\ S\,m^{-1}$ over the same range. The dielectric properties obtained from the DNA suspension of the malignant group were found to be significantly different from those of both the benign and control groups, with the DNA suspension of the malignant group having higher values. While, the dielectric properties were not found to show a significant positive correlation with the grade of the cancer.

4.3.9. Thyroid

Cheng and Fu (2018b) measured the dielectric properties of normal thyroid samples and papillary thyroid cancer samples in the frequency range of 0.5 to 8 GHz using a coaxial probe. All 236 freshly excised thyroid tissues (138 normal and 98 malignant) from 48 patients were measured within 2 h from excision. Post-excision specimen desiccation was minimized by placing specimens in heated, sealed, and insulated containers for transportation to the measurement area. A pathological examination was also conducted to confirm the histological type of each specimen. They found a statistically significant difference between the two tissue types. The measured data for the mean effective dielectric permittivity varied from 4.03 ± 1.95 to 17.95 ± 1.65 and from 69.78 ± 2.73 to 57.36 ± 1.80 (across the frequency range) for the normal and cancerous tissues, respectively. The obtained mean effective conductivity varied from 0.84 ± 0.20 to 1.87 ± 0.10 S m^{-1} and from 1.90 ± 0.50 to 9.75 ± 0.94 S m^{-1} for the normal and cancerous tissues, respectively.

In Gavazzi *et al* (2018), the dielectric properties of normal, benign, and malignant thyroid tissues obtained from surgery were measured from 200 MHz to 10 GHz using a coaxial probe. Twenty-three excised tissue samples were obtained from 14 patients. Specimens were classified into five groups according to a histological examination, mainly normal, struma (nodular goiter), thyroiditis, adenoma, and cancer, and the data showed that the relative permittivity of the normal thyroid tissue was on average 10% lower than that of cancer tissue and 8% lower than that of goiter tissue over the entire frequency range. The percentage difference in conductivity between normal and malignant tissues varied from 21% to 8% and the percentage difference between normal and goiter tissues varied from 14% to 7% up to 2.45 GHz. However, no statistical difference in the conductivity was observed among the different tissue groups at higher frequencies, with no clear difference between benign and malignant tissues.

In Huang *et al* (2021) the differences in the dielectric properties of *in vitro* normal thyroid tissue and benign and malignant thyroid nodules (nodular goiter, follicular adenoma, papillary carcinoma, and follicular carcinoma) were reported. The dielectric properties were measured using a coaxial probe from 1 to 4000 MHz and tissue samples were obtained from 155 patients. Measured data showed that dielectric properties can be correlated to the degree of malignancy, with the 20–70 MHz frequency band giving the most statistically significant difference between the different tissue types. The measured data was also fitted to a two-pole Cole–Cole model.

4.4. Discussion and research needed

Breast and colon tissues have been the most thoroughly studied tissues to date across the microwave and mm-wave (<50 GHz) ranges. For breast tissues, multiple studies have reported data from large patient groups to support imaging applications across these ranges (see table 6). For colon tissues, large studies have similarly been conducted to support tissue-type detection/classification (see table 7). However, in general, the availability of dielectric data measured from human samples is quite limited. No studies reporting data on diseased bulk lung tissue samples were found, nor were works on other key organs such as the stomach, uterus, and brain. Data on benign but abnormal tissues are also rare. Additionally, for many tissues, the data are limited to only one or two studies, including for the prostate, skin, saliva, bladder, and blood (for blood-related cancers and other types of malignancies). Obtaining new dielectric data from human samples, particularly diseased samples, should undoubtedly be a priority of future studies. Studies should include sufficiently large populations to quantify the inter- and intra-patient variability in the dielectric properties, as this information is vital for designing and implementing effective end-use medical technologies.

Furthermore, the frequencies considered in these studies span a wide range from 10 Hz to 50 GHz. However, no single tissue has been characterized across this range. Additionally, new studies are also needed to characterize tissues beyond 50 GHz, through the upper GHz range into the THz range. Further studies with higher frequencies should be a primary area of future research, particularly as THz-range imaging for medical diagnostics and tissue-type classification has become an active area of study (Shi *et al* 2018, Sung *et al* 2018, Chavez *et al* 2020).

In the reviewed studies on breast tissue, different tissue classification resulted in conflicting views on whether a statistically significant contrast in the dielectric properties exists. The study by Sugitani *et al* (2014) highlighted this point further by showing the dependence of such properties on the volume fraction of cells in the measured volume. Therefore, the dielectric data characterisation of malignant tissues and the method of categorising normal and malignant tissues need to be investigated for both breast tissue and other tissues.

Despite the limited data, the evidence to date indicates that for most tissue types, there is a detectable difference between the dielectric values of healthy and malignant tissues. However, as is evident in the above text, this contrast depends on the type of healthy tissue, the type of malignant tissue, and the frequency. This can be seen in the quantitative values for the dielectric properties in the above sections and is demonstrated in figures 5 and 6 for healthy and diseased breast and colorectal tissues, respectively. Furthermore, several studies also

suggest that, in general, there are trends in the dielectric properties with the cancer grade (Ranade *et al* 2016, Li *et al* 2017, Guardiola *et al* 2018). Therefore, these works show promise for future medical diagnostic and therapeutic technologies as they suggest the ability to identify malignancies or discriminate them from healthy tissues and the possibility to classifying the grade or type of malignancy, based on the dielectric properties of tissues.

5. Variability of dielectric properties of tissues due to measurement-specific conditions

As shown in the previous sections, the dielectric measurements of tissues have been conducted by an invasive approach: the dielectric properties were derived from electromagnetic responses resulting from placing a probe or electrode terminal(s) in contact with the tissues, and excised tissues were used in most cases. The dielectric properties of tissues in the living state are the main concern in electromagnetic modeling of the human body. However, the conditions under which the measurement in the intended state can be realized are limited, and alternative approaches under well-controlled conditions have been employed, such as by using animal subjects or conducting measurements at room temperature. Moreover, even if the measurement is performed in the intended state, it may not always be possible to conduct dielectric measurements reproducibly owing to the difficulty of controlling the tissue conditions. Therefore, this section summarizes studies that report variations in the dielectric properties of tissues due to the measurement-specific conditions.

5.1. Postmortem effects
This section focuses on changes in dielectric properties due to postmortem, in other words, on the difference between *in vivo* and *in vitro* measurements. In addition, variations with the time when the measurements took place (postmortem time) are also included in this review.

5.1.1. Low- and intermediate-frequency domain (below 10 MHz)
Gabriel *et al* (1996b) presented the dielectric properties of human tongue *in vivo* from 2 MHz to 20 GHz, and compared them with their data measured *in vitro* for human, ovine, and porcine subjects. They demonstrated that the difference tends to increase with decreasing frequency below 100 MHz, although no significant differences were observed at higher frequencies.

Haemmerich *et al* (2002) investigated the postmortem effects on the resistivity of swine liver *in vivo* and *in vitro* from 10 Hz to 1 MHz. They observed an increase in resistivity (decrease in conductivity) of up to approximately 60% in 10 min after the liver blood supply had occluded (ischemia). Then the change in the resistivity of the liver was measured up to 12 h after excision and compared with the data obtained *in vivo*. They observed an increase in resistivity of 30%–80% compared with the data obtained *in vivo* for up to 2 h; the variation tended to exceed 50% below 1 kHz. Authors commented that although the decrease in tissue temperature from 38 °C to around 22 °C was one of the causes of the increase, the ischemia also increased the resistivity. After 2 h, a decrease in the resistivity was observed, which was assumed to be due to cell membrane breakdown of the tissue. The values of resistivity 12 h after from excitation were slightly higher than those obtained *in vivo*, and the differences were around 10%–20%, thus comparable to the effect of temperature change from 38 °C to 22 °C, as estimated by the authors.

Zurbuchen *et al* (2010) compared the conductivity of porcine liver obtained by *in vivo* and *in vitro* measurements at 470 kHz. They found that the conductivity at 37 °C measured *in vivo* was approximately 34% higher than that *in vitro*.

Wang *et al* (2015) investigated the postmortem effect of human liver *in vitro* obtained from 20 patients (49 ± 12 years of age) at frequencies from 10 Hz to 100 MHz. Tissues were maintained at 37 °C with humidity of 90% after surgery and the postmortem effect was investigated from 15 min to 24 h after excision. No postmortem change in permittivity was observed, but a significant change in conductivity was observed from 15 min to 24 h after excision at frequencies below 1 MHz. The conductivity tended to decrease up to 1 h after excision, and then increased up to 24 h after excision. The conductivities at 500 Hz and 2 MHz after an excision time of 24 h were 130 and 50% higher than those measured 15 min after excision, respectively. The authors commented that because of the dispersion characteristics, the postmortem effect on the dielectric properties was less sensitive above 1 MHz than at lower frequencies.

5.1.2. Radiofrequency domain (over 10 MHz)
Schmid *et al* (2003a) reported postmortem changes in the dielectric properties of porcine brain grey matter in the frequency range of 800–1900 MHz. The number of subjects was 10 and postmortem changes were observed up to 60 min after sacrificing the animals. The postmortem effect was observed with a tissue temperature of 38 °C by correcting the measured dielectric properties using their temperature dependence based on

temperature coefficients obtained by separate *in vitro* measurements of porcine brain. At frequencies of 0.9 and 1.8 GHz, decreases in permittivity and conductivity of 4% and 8%–12%, respectively, were observed at a postmortem time of 60 min. The obtained postmortem changes were less than twice the maximum combined standard uncertainty of the measurement.

Peyman *et al* (2007) compared the dielectric properties of porcine brain tissues obtained by *in vivo* and *in vitro* measurements from 50 MHz to 20 GHz. The measurements were conducted with an average tissue temperature of approximately 37 °C. For grey matter, little difference in the dielectric properties was observed between the *in vivo* and *in vitro* measurements, with the difference within the combined uncertainty of the measurements in the measured frequency range. On the other hand, the differences were within twice the combined uncertainty for white matter; the maximum combined uncertainties were reported to be below 6% and 8% for permittivity and conductivity, respectively, in the measured frequency range. Authors noted that it is difficult to identify the systematic cause of the differences from the comparison between dielectric properties obtained by *in vivo* and *in vitro* measurements. They also commented that it is essential to avoid drying of tissue samples and that differences in the dielectric properties may not be observed between *in vivo* and *in vitro* measurements at microwave frequencies.

Lazebnik *et al* (2007a, 2007b) investigated postmortem changes in the dielectric properties of human breast tissues collected by reduction and cancer surgeries from 50 MHz to 20 GHz. The dielectric properties measured up to 50 min and 250–300 min after excision were compared for each category of breast tissue. They observed a statistically significant decrease in the dielectric properties over time after the excision of tissues with high adipose content collected from reduction surgery, but desiccation was considered as the cause of the change. Similarly, Martellosio *et al* (2017) found no significant differences between those with postmortem times below and more than 90 min for both tumourous and normal human breast tissues in the frequency range from 0.5 to 50 GHz.

O'Rourke *et al* (2007) compared the dielectric properties of human liver tissues measured *in vivo* and *in vitro* at 915 MHz and 2.45 GHz collected from five patients who underwent hepatic resection. The *in vitro* measurements were conducted approximately 30 min after excision and at tissue temperatures of 20 °C–24 °C. Measured values obtained *in vitro* showed a decrease in dielectric properties of up to 30% compared with those measured *in vivo*.

Farrugia *et al* (2016) compared the dielectric properties of rat liver obtained by *in vivo* and *in vitro* measurements from 500 MHz to 40 GHz. Both *in vivo* and *in vitro* measurements were conducted at a tissue temperature of around 37 °C. They reported slight changes in the dielectric properties after excision, which were comparable to or smaller than the experimental uncertainty. From the obtained results, they concluded that measurements using excised tissues accurately simulate those of living tissues in the considered frequency range, provided that the tissues are kept well hydrated and at body temperature.

Pollacco *et al* (2018) compared the dielectric properties of rat muscle and fat measured *in vivo* and *in vitro* from 0.5 to 50 GHz. The *in vitro* measurements were conducted at a tissue temperature of 25 °C. A slight decrease in the dielectric properties from those measured *in vivo* was observed for the *in vitro* measurements, and the difference was comparable to the combined uncertainty in the measurements. They also investigated the effect of dehydration on the dielectric properties of the tissue measured *in vivo*, and a large decrease in the dielectric properties was observed with the dehydration of both muscle and fat tissues. They concluded that excised tissues reliably represent the dielectric parameters of *in vivo* tissues under certain controlled hydration conditions.

Sabouni *et al* (2020) compared the dielectric properties of murine colonic tumours obtained by *in vivo* and *in vitro* measurements. The measurements were conducted at frequencies from 1 to 5 GHz, and the tissue temperatures ranged from 27 °C to 33 °C and from 20 °C to 25 °C for the *in vivo* and *in vitro* measurements, respectively. The dielectric properties obtained *in vivo* were higher than those obtained *in vitro*, which was due to the changes in the tissue temperature and water content.

5.2. Animal species and human race/gender

5.2.1. Animal species

Potential differences between the dielectric properties of human and animal tissues have also been a topic of interest to researchers. However, there are a limited number of studies in which measurements of both human and animal tissues were carried out. Gabriel *et al* (1996b) compared the dielectric properties of tongue and adipose tissues between humans and other mammals at frequencies from 10 Hz to 20 GHz. In addition, they performed comparisons between animal species for cartilage and cortical bone. Their results demonstrated that the difference between individuals of each species may exceed the variation between species.

Intercomparisons of literature values made in different studies were summarized in section 3 (e.g. figures 2–4), and systematic differences in tissue conditions, such as heterogeneity, temperature, and water contents, were

often suggested as the cause of the observed discrepancies, and no indication of a systematic difference between different species according to the data summarized in the previous sections.

5.2.2. Human race/gender

Differences in skin permittivity by gender and race were discussed by Mayrovitz *et al* (2010, 2012, 2015, 2016), who performed *in vivo* measurement of human skin at 300 MHz. They observed a difference of more than 20% in permittivity with respect to gender for several body parts. A cause of the difference in permittivity was specified as the gender difference in skin thickness, implying that the derived permittivity was affected by adipose tissue below the skin that owing to the sensing depth of the coaxial probe. Regarding race dependence, values of permittivity measured *in vivo* from skins of 100 volunteers of five different races (10 male and 10 female volunteers for each race) were compared, and a maximum difference of around 20% was observed among the races. However, their reported data showed that the race difference was smaller than the gender difference, which was expected from the greater gender difference than race difference in skin thicknesses. Moreover, the differences were comparable to the standard deviations of the volunteers for each race and gender.

5.3. Aging

With the development of anatomical computational models for children (Dimbylow 1997, Lee *et al* 2005, Nagaoka *et al* 2008, Christ *et al* 2010), studies on the age dependence of dielectric properties have been conducted since the early 2000s. These studies were conducted for the frequencies of radio communication technologies, i.e. 50 MHz to 50 GHz, and findings for each tissue type are summarized as follows.

5.3.1. Brain tissues

Schmid and Überbacher (2005) investigated the age dependence of dielectric properties for bovine white and grey matter from 0.4 to 18 GHz. The dielectric properties of adult (16–24 months) and young (4–6 months) animals were compared, and decreases in the dielectric properties with age were found for white matter but not for grey matter. The authors explained this by suggesting that aging may change the water content of white matter tissue through a physiological process. Similar observations were made by Peyman *et al* (2007) and Mohammed *et al* (2016), who investigated the effect of aging for porcine tissues at frequencies from 50 MHz to 20 GHz and for canine tissues at frequencies from 0.3 to 3 GHz, respectively.

    Peyman *et al* (2007, 2009) reported decreasing dielectric properties with aging for spinal cord and dura from a comparison of porcine tissues aged around 35, 100, and 600 d with masses of 10, 50, and 250 kg, respectively. Similarly to white matter, the effect of aging was explained by the increase in myelination and the decrease in water content. For dura, the aging effect was explained by a decrease in the influence of the surrounding cerebrospinal fluid on the measured dielectric properties due to the increasing dura thickness with age.

    In addition to examining white and grey matter, Mohammed *et al* (2016) compared cerebrospinal fluid at room temperature collected from dogs with ages of 20–81 months, and no significant variation in the dielectric properties with age was observed.

5.3.2. Bone tissues

Peyman *et al* (2009) reported decreasing dielectric properties with age for several bone tissues, i.e. cortical bone, skull, and bone marrow. For bone marrow, the shift of contents from red marrow to yellow marrow with age was considered as the cause of the aging effect. For cortical bone and skull, the reduction in water content and the increase in calcification with age are the cause of the aging effect on the dielectric properties. A similar aging effect was observed for a canine skull by Mohammed *et al* (2016).

5.3.3. Eye tissues

The aging effect on the dielectric properties of the cortical lens was reported by Schmid and Überbacher (2005), and the observed differences were explained as a consequence of the dynamic process in lens development with age. On the other hand, investigations for the cornea and vitreous humor did not show significant age effects on the dielectric properties of the investigated mammalian eye tissues (Schmid and Überbacher 2005, Peyman *et al* 2009).

5.3.4. Skin

Aging effect on the dielectric properties of skin were investigated by Peyman *et al* (2009) and Mayrovitz *et al* (2017). Mayrovitz *et al* (2017) investigated the aging effect on the permittivity of human skin measured *in vivo* at 300 MHz using several coaxial probes with different sensing depths from 0.5 to 5 mm. Significantly higher values for permittivity (around 20%) were reported for the age group of 62–92 years than for a group of younger individuals (below 56 years of age) when a coaxial probe with a sensing depth of 0.5 mm was used. Considering

Table 9. Overview of review results on image-based estimation of dielectric properties of human tissues measured *in vivo*.

Author	Frequency	Tissues	Notes
Voigt *et al* (2011)	64 MHz	Brain (6 subjects)	MREPT (conductivity and permittivity)
van Lier *et al* (2012)	298 MHz	Head	B_1^+ phase 7 T MRI (conductivity)
Kim *et al* (2014)	128 MHz	Brain (1 subject)	3 T MRI (conductivity and susceptibility)
Shin *et al* (2015)	128 MHz	Breast (90 subjects)	3 T MREPT (conductivity)
Lee *et al* (2016)	128 MHz	Breast and brain	3 T MREPT (conductivity)
Gho *et al* (2016)	128 MHz	Brain (3 subjects)	UTE (conductivity and susceptibility)
Dabek *et al* (2016)	2–127 Hz	Head (9 subjects)	EIT-EEG (conductivity)
Katoch *et al* (2019)	128 MHz	Brain (5 subjects)	3 T MRI (conductivity tensor)
Gavazzi *et al* (2020a)	RF and other frequencies	Brain (3 subjects)	3 T MRI (conductivity)
Sun *et al* (2020)	128 MHz	Brain (1 + 2 subjects)	MRI (conductivity) – wavelets/TV
Marino *et al* (2021)	128 MHz	Brain (5 subjects)	3 T MRI (conductivity tensor)
Lee *et al* (2021)	1 kHz/5 MHz	Brain (3 subjects)	3 T MRI (conductivity tensor)
Jahng *et al* (2021)	1 kHz/5 MHz	Brain (1 subject)	3/9.4 MRI (conductivity tensor)
Mandija *et al* (2019)	128 MHz	Head (3 subjects)	MREPT (conductivity and permittivity) – deep learning
Hampe *et al* (2020)	128 MHz	Brain (14 + 18 subjects)	3 T MRI (conductivity) – deep learning
Gavazzi *et al* (2020b)	128 MHz	Pelvic (42 subjects)	3 T MRI (conductivity) – deep learning
Rashed *et al* (2020a)	10 kHz	Head (8 subjects)	3 T MRI (conductivity) – deep learning
Rashed *et al* (2020b)	0.9, 1.8 and 3.0 GHz	Head (8 subjects)	3 T MRI (conductivity and permittivity) – deep learning
Sajib *et al* (2021)	100 Hz	Brain (1 subject)	DT-MREIT (conductivity tensor) – machine learning

the fact that no age dependence was observed when the sensing depth was larger than 1.5 mm, the authors stated that the change in skin water from a bound state to a more mobile state for the elder group is the cause of the aging effect on the dielectric properties of skin.

5.3.5. Adipose tissues

Several studies investigated the aging effect on the dielectric properties of adipose tissues. Peyman *et al* (2009) focused on porcine fat, and Lazebnik *et al* (2007a;2007b) and Martellosio *et al* (2017) focused on normal human breast tissues collected by reduction or cancer surgeries. Only Martellosio *et al* (2017) reported an aging effect on the dielectric properties: a significant difference was found between the groups with ages below 40 years and above 60 years for the tissues with a high adipose content of above 80%, i.e. tissues with low dielectric properties. However, the effect of age was much smaller than the variation of the dielectric properties with the adipose content observed for normal adipose tissues (see section 3.2).

5.3.6. Other tissues

Peyman *et al* (2009) also investigated the age dependence of the dielectric properties for intervertebral disc, periosteum, and tongue. No significant effect of age was observed for tongue but decreasing dielectric properties with the age of tissues were observed for intervertebral disc and periosteum, and the decrease in the water content with age was given as an explanation for the age effect.

Lazebnik *et al* (2007b) discussed the aging effect on the dielectric properties for malignant human breast tissue measured *in vitro* at 5, 10, and 15 GHz, and no statistical significance was found for the aging effect on the dielectric properties.

5.4. Discussion and research needed

Several studies have investigated differences in dielectric properties between *in vivo* and *in vitro* measurements and/or the postmortem effect on dielectric properties. To date, the reasons given for the considerable systematic postmortem changes are the effects of stopping blood circulation (ischemia), breakdown of the membrane in the tissue, and the tissue temperature. Precise measurements on liver tissue at frequencies below 1 MHz by Haemmerich *et al* (2002) demonstrated that two of these effects caused the measurement results to change in opposite directions: ischemia led to a decrease in conductivity, and breakdown of the membrane led to an increase in conductivity. From these observations, it is recommended that these two systematic factors are considered separately, especially since it has been reported that the factor due to breakdown of the membrane varies with the time from excision. In addition, it is essential to pay particular attention to changes over time when measuring excised tissue samples at frequencies below 1 MHz. At higher frequencies, the postmortem effect is smaller than that below 1 MHz. In particular, little effect of breakdown of the membrane is expected because of the reduced impact of α- and β–dispersions in the radiofrequency domain. In fact, the results of intercomparison between reported data for each skin (figure 2(a)) and brain tissues (figures 4(a) and (b)) demonstrated good agreement between dielectric properties measured *in vivo* and *in vitro*. Several authors

commented that *in vitro* measurement of tissues at radio and microwave frequencies can accurately simulate the dielectric measurement of tissues *in vivo* provided the tissue temperature is maintained at body temperature and the tissue is prevented from drying (Peyman *et al* 2007, Farrugia *et al* 2016, Pollacco *et al* 2018). In the future, the development of standardized tissue handling and measurement processes and metadata recording procedures may also help enable the comparison of data across studies (Porter and O'Halloran 2017).

Regarding the differences in the dielectric properties between animal species, differences in the cellular structure and tissue composition are possible factors that can impact the dielectric properties. According to current knowledge, there is no objective reason why animal tissue cannot be used as a substitute for human tissue. In particular, in the radiofrequency region, the intercomparison of data between published studies demonstrates the consistency in data between human and animal subjects. On the other hand, intercomparison of data (such as by Gabriel *et al* (2009)) showed a larger spread of the data below 1 MHz than that at higher frequencies. In general, for detailed investigations concerning the variability of dielectric properties due to the measurement-specific conditions of tissues, it is essential to rigorously assess the measurement uncertainty.

Regarding the aging effect on dielectric properties, investigations in the frequency range from 50 MHz to 50 GHz have been reported. Changes in the composition/component, such as the water content in the tissue, with growth and aging are the main causes of the aging effect. Measured dielectric properties of animal tissues with respect to age were parameterized by Peyman and Gabriel (2010) on the basis of measurements by Peyman *et al* (2009). Although appropriate age conversion from data obtained on animal tissues to the human case is necessary, the dielectric properties can be adopted in anatomical models of children. However, data are scarce at frequencies below 50 MHz and above 50 GHz. The age-dependent variations in the cellular structure and water content have been reported as the potential cause of the variation in the dielectric properties at lower frequencies. Moreover, the variation in the water content in the tissue with growth may affect the dielectric properties at higher frequencies.

6. Recent advances in image-based estimation of dielectric properties

Non-invasive dielectric measurements of human tissues provide useful information for several clinical applications such as diagnosis of abnormalities and identification/characterization of sensitive tissues. Moreover, they play a basic role in electromagnetic stimulation studies such as on brain stimulation as well as in human exposure assessments. The term EPT (Electrical Properties Tomography) refers to the acquisition of an RF-induced magnetic field through an RF coil located within an MRI scanner. In this section, we report a systematic search of the literature on dielectric measurements using EPT that was undertaken using Web of Science (Oct. 2021); details of the search terms are given in appendix A. In total, the 18 papers listed in table 9 were found, and major and recent developments in EPT with a focus on human *in vivo* studies are summarized.

6.1. Review of dielectric properties
Dielectric properties can be acquired through several techniques such as electrical impedance tomography (EIT), magnetic induction tomography (MIT), magnetic resonance electrical impedance tomography (MREIT), and several others. In the following, major contributions are reviewed.

6.1.1. Electrical properties tomography (EPT)
A 3D brain mapping that obtained dielectric properties from a standard MRI scan in a few minutes was reported by Voigt *et al* (2011). Data acquired from six healthy male volunteers were used to validate the dielectric properties of brain tissues at 64 MHz. A large variation was observed in the values obtained for grey matter, white matter, and cerebrospinal fluid (conductivities of 0.69 ± 0.14, 0.39 ± 0.15, and 1.75 ± 0.34 S m^{-1} and relative permittivities of 103 ± 69, 72 ± 64, and 104 ± 21, respectively), although consistency with the results of simulation studies was obtained from many perspectives.

In another study by van Lier *et al* (2012), the propagating B_1^+ phase was used to measure the electrical properties of human head tissues at 298 MHz. By using the homogenous Helmholtz wave equation, a good estimation of tissue conductivity was possible, and results were confirmed using electromagnetic simulation studies. The measured conductivities of grey matter, white matter, and cerebrospinal fluid were reported to be 0.87 ± 0.21, 0.63 ± 0.27, and 1.93 ± 0.2 S m^{-1}, respectively.

Kim *et al* (2014) reported that the simultaneous acquisition of electrical conductivity and magnetic susceptibility was possible through a 3D multiecho gradient-echo sequence. Results from phantom and brain imaging with 3 T MRI at 128 MHz demonstrated the feasibility of this approach.

In another clinical application, the electrical conductivity of 90 subjects was measured at 128 MHz for breast cancer diagnosis by Shin *et al* (2015). The results showed remarkable differences in the measured electrical

conductivities of parenchymal tissue (0.43 S m^{-1}) and fat (0.07 S m^{-1}) compared with those in benign (0.56 S m^{-1}) and malignant (0.89 S m^{-1}) regions, which demonstrate efficient usage for breast cancer diagnosis.

Lee *et al* (2016) developed a multi-receiver coil approach to reconstruct conductivity using MR imaging. The results demonstrated that their method can reduce the variation in conductivity (<15%) and suppress artifacts. The estimated conductivity values were 0.40 $\pm$ 0.13 and 2.16 $\pm$ 0.32 S m^{-1} for grey/white matter and cerebrospinal fluid, respectively.

Gho *et al* (2016) extended the method proposed by Kim *et al* (2014) by reducing the required time and improve the sensitivity to motion artefacts. *In vivo* measurements were conducted for of three healthy adult volunteers. The reported conductivities of grey matter, white matter, and cerebrospinal fluid were 0.68 $\pm$ 0.06, 0.36 $\pm$ 0.05, and 2.20 $\pm$ 0.13 S m^{-1}, respectively, at 128 MHz.

6.1.2. Electrical impedance tomography (EIT)

Electrical impedance tomography has been known since the work of Henderson and Webster (1978). It was also referred to as applied potential tomography (APT) in early studies (Brown *et al* 1985). Although the use of the homogenous Helmholtz equation is common for EPT, a method that combines Maxwell's integral equation and high-permittivity materials to improve the estimation quality was proposed by Schmidt and Webb (2016).

Dabek *et al* (2016) adopted another method based on EIT with electroencephalography and it was used to estimate the electrical conductivity of head tissues of nine subjects at frequencies from 2 to 127 Hz. Data measurements using a 64- electrode electroencephalography layout with consideration of background measurements were performed to estimate the conductivity of the scalp, brain, and skull. The results demonstrated a large inter-subject variability of conductivity from 11 to 127 Hz (skull: 6.7 $\pm$ 6.2%, scalp and brain: 1.6 $\pm$ 2.0%).

6.1.3. Magnetic resonance electrical impedance tomography (MREIT)

A conductivity tensor is usually used to demonstrate the anisotropic electrical properties of tissues. This explains why conductivity tensor imaging (CTI) is another common name used for MREIT. Diffuse tensor magnetic resonance electrical impedance tomography (DT-MREIT) exhibits values that highly match those measured using invasive methods (Jeong *et al* 2017). This method enables the direction of water mobility and the ion concentration to be acquired and images of anisotropic tensor conductivity to be generated.

Katoch *et al* (2019) demonstrated the results of using a 9.4/3 T MRI scanner for electrodeless CTI of a phantom and the human brain of 5 subjects. The human subjects were imaged with 3 T MRI at 128 MHz and the results demonstrated significant inter-subject variabilities. CTI method might be of clinical use as it can be used with a clinical MRI scanner without additional hardware. The reconstructed conductivities were in the ranges of 0.2–0.3, 0.08–0.27, and 1.55–1.82 S m^{-1} for grey matter, white matter, and cerebrospinal fluid, respectively. The anisotropy ratios of grey matter and white matter were 1.12–1.19 (mean = 1.16) and 1.96–3.25 (mean = 2.43), respectively.

Gavazzi *et al* (2020a) developed a method named PLANET for the reconstruction of transceiver phase maps, which was validated as a potential method for electrical conductivity mapping using a phantom and volunteer subjects. This method demonstrated efficiency in handling the partial volume effect, and conductivity values of whole brains were reported.

Sun *et al* (2020) utilized signal processing techniques such as total variation and wavelet regularization which was used to enhance the accuracy of conductivity maps of brain tissues at 128 MHz. The results demonstrated the elimination of the noise effect in conductivity maps, and conductivity values of 0.69 $\pm$ 0.09, 0.43 $\pm$ 0.05, and 1.82 $\pm$ 0.35 S m^{-1} were obtained for grey matter, white matter, and cerebrospinal fluid, respectively.

Marino *et al* (2021) calculated CTI maps by combining high frequency conductivity derived from water maps and multiple b-value DTI from the brain data of five subjects. The computed conductivity tensor demonstrated values of 0.55 $\pm$ 0.01, 0.3 $\pm$ 0.01, and 2.15 $\pm$ 0.02 S m^{-1} for grey matter, white matter, and cerebrospinal fluid, respectively, at 128 MHz. The coefficient of variation was computed from the isotropic conductivity distribution and showed large inter-subject variability even with a small number of subjects. The authors recommended not to use these values as references for further studies.

Lee *et al* (2021) developed a method based on a two-compartment model to convert the high-frequency conductivity into the extracellular medium conductivity. Results from three subjects and a phantom demonstrated that the proposed method could reconstruct the extracellular electrical properties from the high-frequency conductivity using standard MRI scans. The mean conductivities of grey matter, white matter, and cerebrospinal fluid of the three subjects at 5 MHz were around 0.5–0.6, 0.4, and 1.5 S m^{-1}, and the relative standard deviations from the mean were in the range of 49%–59%, 38%–48%, and 42%–57%, respectively.

Jahng *et al* (2021) developed a multi-compartment model with the B1 mapping technique to reconstruct the conductivity tensor in phantom, animal, and human studies. A single healthy female subject was used in this study, and the results demonstrated that the proposed model has the potential to estimate the conductivity

tensor without external current injection. The conductivities of grey matter, white matter, and cerebrospinal fluid were reported to be 0.59 ± 0.09, 0.42 ± 0.05, and 1.59 ± 0.44 S m^{-1} at 128 MHz and 0.52 ± 0.08, 0.27 ± 0.05, and 1.56 ± 0.46 S m^{-1} below 1 kHz, respectively.

6.1.4. Artificial intelligence with imaging approach

Learning-based methods have demonstrated a significant improvement in several data processing/signal analysis applications.

Mandija *et al* (2019) made it possible to estimate the dielectric properties of human head tissues through a generalized adversarial network (GAN). The results for three subjects demonstrated a remarkable improvement compared with those obtained by conventional MR-EPT methods at 128 MHz. The conductivities were estimated to be 0.53 ± 0.18, 0.37 ± 0.04, and 1.67 ± 0.47 S m^{-1} for grey matter, white matter, and cerebrospinal fluid, and the corresponding relative permittivities were reported to be 66.0 ± 6.9, 54.4 ± 3.2, and 80.1 ± 4.9, respectively.

Hampe *et al* (2020) discussed potential extensions of deep learning EPT techniques using a patch-based U-net architecture and their applications. They investigated data obtained from 14 patients and 18 healthy subjects. The validity of deep learning in estimating brain conductivity mapping at 128 MHz was demonstrated.

Gavazzi *et al* (2020b) adopted deep learning in estimating the conductivity of human pelvic from 42 subjects at 128 MHz. The deep learning conductivity estimation showed high accuracy (average mean error of less than 0.1 S m^{-1}). A 3D patch-based convolutional neural network (CNN) used the transceive phase and B_1^+ to estimate electrical conductivity. The highres3dnet architecture was considered as the backbone network for this study, and the results demonstrated high performance compared with conventional methods.

Rashed *et al* (2020a) presented a deep learning architecture named CondNet as a network architecture that can effectively estimate a non-uniform conductivity map using T1/T2-weighted MRI. The Conductivities of eight tissues, i.e. cerebrospinal fluid, vitreous humor, fat, grey matter, mucous, skin, bone (cortical) and white matter, at 10 kHz obtained from image data of eight subjects were reported. The results demonstrated the efficiency of the proposed method in handling inter- and intra-subject variabilities by estimating the conductivity of whole-head tissues.

Later on, Rashed *et al* (2020b) extended CondNet to estimate the conductivity, permittivity, and density of 12 head tissues, i.e. blood, cancerous bone, cortical bone, grey matter, white matter, cerebellum, cerebrospinal fluid, dura, fat, mucous, skin, and vitreous humor, of eight subjects at 0.9, 1.8, and 3 GHz in studies on energy absorption by RF exposure. Dielectric properties and those variations (standard deviations) were also reported. They observed large variations (relative standard deviations from mean) for tissues with low dielectric properties, such as bone tissues and fat.

Sajib *et al* (2021) utilized a machine learning approach to reduce the number of injected current patterns in the DT-MREIT technique to a single pattern. The results of their phantom and human experiments demonstrated a small error of within 15% at 100 Hz.

6.2. Limitations

Image-based estimation of dielectric properties provides a useful non-invasive techniques that enable several clinical applications such as cancer diagnosis, subject-specific tissue mapping, and neurostimulation. While EPT provides a feasible approach for dielectric property acquisition, it suffers from the common challenges known for tomographic imaging mainly related to solving the inverse problem. MRI acquisition with high quality requires a considerable time with potential artifacts expected with minor subject movements (Zhang *et al* 2014). Moreover, image-based methods usually requires a special acquisition protocols and sophisticated hardware that may increase the acquisition cost. On the other hand, as we reviewed above, the quality of the estimation of dielectric properties still lacks accuracy and the range of uncertainty is still large. It is still challenging to clearly and efficiently validate the accuracy of different approches.

Deep learning methods are emerging to be a method of choise due to their ability to learn from relatively large datasets. Data-driven models can efficiently solve several problems associated with the inter- and intra-subject variabilities. However, in most cases, deep learning architectures are provided as black-box, making it almost impossible to validate the process and analyze the reconstruction of the dielectric properties. Also, optimization of the network architecture and parameter selection are commonly done using time-consuming ablation studies.

6.3. Discussion and research needed

The dielectric properties of living tissues are associated with several medical and industrial applications. The requirement of fast, accurate, robust, and low-cost methods would keep this research track open for a while. Current image-based methods discussed in the previous sections can lead to good average values but still within

large variations. More accurate methods with a narrow error range can lead to higher accuracy in electromagnetic applications such as radiation safety and neuromodulation. Moreover, image-based methods are known to suffer from challenges associated with imaging protocols and the modalities used. For example, in many cases, subjects with metal implants can lead to sigificant artefacts in the formulated images and therefore, it reduce the fesability of dielectric properties estimated for these subjects. Other challenging associated with imaging, such as statistical noise, motion artefacts, and hardware calibration errors, can also be difficult to handle. Therefore, advances of this track is highly associated with the development of imaging technology.

7. Summary

This paper systematically reviewed the dielectric properties of biological tissues based on our search strategy. Although the 1996 database focused on frequencies up to 20 GHz and general tissues, this review extended the frequency range up to 1 THz by considering modern trends in the electromagnetic modeling of the human body. It also provided an intercomparison of reported data for several tissues and a comparison with data from the database extrapolated to the higher frequencies. In addition, a summary of the differences between the dielectric properties of healthy and malignant tissues was given for many tissue types and demonstrated detectable dielectric differences for most tissue types. The factors impacting the dielectric properties of tissues were discussed, covering wide ranges of frequencies and tissue types. As topics of recent interest in dielectric measurement, the image-based estimation of dielectric properties and the use of artificial intelligence technologies were included in this review, and findings for the *in vivo* measurement of humans were summarized. We also outlined further studies required in each topic covered in this review for future advances in the electromagnetic modeling of the human body, which are essential in the research fields of human protection from non-ionizing radiation and biomedical applications.

Acknowledgements

Appendix A. Search strategies for systematic review

This appendix shows the search criteria we employed when using search engines for our systematic review. General inclusion criteria included the following: published in peer-reviewed journal publications, not review paper, reporting measured dielectric data of tissue, frequencies up to 1 THz, and published from 1996 to the time of writing this review. Further details of the search terms and additional criteria are as follows.

For the search strategy for general tissues, the search was undertaken using the keywords shown in table A1 using Web of Science (August 2021). Studies on dielectric measurement with image-based estimation methods were excluded and searches were undertaken separately as shown below. All papers reporting measurement data of tissues were additionally extracted for section 3. In addition, papers cited in the extracted papers that met the scope of the section were included. The search results for general tissues were also utilized to extract papers focusing on the variability of the dielectric properties of tissues for section 5 and appendix B.

For malignant tissues, a search was undertaken using the keywords shown in table A2 using three search engines: Web of Science, PubMed, and Google Scholar (Aug. 2021). Papers reporting dielectric measurements from human or human-derived samples of malignant tissues were extracted for section 4.

For the image-based estimation of dielectric properties, a search was undertaken using the keywords shown in table A3 using Web of Science (Oct. 2021). Papers reporting dielectric properties of human tissues measured *in vivo* were additionally extracted for section 6.

Table A1. Search terms for the dielectric measurement of general tissues (utilized in sections 3 and 5 and appendix B).

1	Any in title	biological* OR tissue* OR organ* OR liver OR muscle OR adipose OR fat OR skin OR breast OR brain OR derm* OR vivo OR rat OR porcine OR bovine OR human
2	Any in all fields	dielectric propert* OR permittivit* OR conductivit* OR dielectric character* OR dielectric measure* OR dielectric spectrum*
3	Any in topic	electromagnetic OR frequenc* OR Hz OR *wave OR *hertz
4	Any in abstract	measure* OR character* OR experiment*
5	Not in title	numerical model* OR human model* OR computational model* OR membrane OR phantom* OR imag* OR detection OR stimulation* OR cell
6	Not in topic	chemi* OR membrane*
7	Not in all fields	seed* OR plant* OR thermal conduc* OR soil* OR food* OR film OR phantom* OR organic*

Table A2. Search terms for the dielectric measurement of malignant and benign tissues (utilized in section 4).

1	Any in title	cancer, tumo*, malignan*, carcinoma, melanoma, adenoma, adenocarcinoma, benign
2	Any in title	dielectric properties, dielectric measurement, dielectric spectroscopy, dielectric characteri*, permittivit*, dielectric constant*

Table A3. Search terms for image-based estimation of dielectric properties (utilized in section 6).

1	Any in title	dielectric propert* OR conductivity OR permittivity
2	Any in topic	human OR body OR tissue OR anatomic
3	Any in topic	mri OR ct OR ultrasound
4	Any in all fields	non-invasive OR *in vivo*
5	Any in all fields	measurement OR acquisition OR imaging

Appendix B. Dependence of dielectric properties of tissues on temperature

The dielectric properties of tissues are dependent on their temperature. However, dielectric measurements of tissues have often been conducted at tissue temperatures lower than those of interest, such as a specific body temperature or higher temperatures (e.g. for thermal therapy). As a recent advance in the dielectric modeling of tissues, a novel empirical equation that takes the temperature variability of the dielectric properties of skin into account has been proposed (e.g. Vilagosh *et al* 2019). This appendix outlines studies in which the dielectric properties of tissues at several temperatures were investigated. The temperature coefficient, i.e. the change in dielectric property per unit temperature increase [% per °C], is often used as a metric and to compensate tissue dielectric properties. The temperature coefficients reported or calculated from the data are summarized as follows.

The temperature coefficients of lung tissue have been examined in detail at temperatures of up to around 100 °C for thermal applications in the medical field. At frequencies from 5 to 500 kHz, the temperature coefficients range from +0.4 to +1% per °C and 1 to 2% per °C for permittivity and conductivity, respectively; these values are based on measurements using porcine liver at tissue temperatures of up to 50 °C by Zurbuchen *et al* (2010) and Yero *et al* (2018). Lazebnik *et al* (2006) reported the temperature coefficients of bovine and porcine livers at frequencies from 0.5 to 20 GHz and developed corresponding parametric models in which Cole–Cole parameters were represented as functions of temperature. According to their parametric models, the temperature coefficients ranged from −0.1 to +0.5% per °C and from −0.4 to +0.8% per °C for permittivity and conductivity, respectively, at 37 °C. These temperature coefficients were of a similar order to those of bovine liver at 915 GHz reported by Chin and Sherar (2001), that is, −0.1% per °C for permittivity and +1.8% per °C for conductivity.

Bao *et al* (1997) measured the dielectric properties of rat white and grey matter at room and body temperatures at frequencies from 0.1 MHz to 25.5 GHz. The calculated temperature coefficients of grey matter were from −0.4 to +2% per °C for permittivity and from −2 to +2% per °C for conductivity. Schmid *et al* (2003a) reported the temperature coefficients of grey matter of porcine brain at 0.9 and 1.8 GHz, which were within the range reported by Bao *et al* (1997). The temperature coefficients for white matter reported by Bao *et al* (1997) ranged from −0.4 to +5% per °C and from −2 to +4% per °C for permittivity and conductivity, respectively, and relatively large values were observed between 0.1 and 10 MHz.

Baumann *et al* (1997) reported the conductivity of human cerebrospinal fluid at 25 and 37 °C from 10 Hz to 10 kHz. The temperature coefficient was approximately +2% per °C. Sasaki *et al* (2015) measured the dielectric properties of the aqueous humor of porcine eye and rabbit cornea at several temperatures from 20 to 35 °C at frequencies from 0.5 to 110 GHz. The calculated temperature coefficients of the aqueous humor were from −1 to +2% per °C for permittivity and ±2% per °C for conductivity, and the corresponding values of the cornea were from −2 to +1% per °C for permittivity and −1 to +3% per °C for conductivity.

Pop *et al* (2003) reported the temperature dependence of the dielectric properties of porcine fat and kidney tissues at 460 kHz. The temperature coefficients of both kidney and fat were +1 and +2% per °C for permittivity and conductivity, respectively.

Chin and Sherar (2004) reported changes in the dielectric properties of rat prostate tissue at 915 MHz. The temperature coefficients were −0.3 and +1% per °C for permittivity and conductivity, respectively.

Appendix C. Tables comparing extrapolated dielectric properties obtained from empirical equations in database and measured dielectric properties over 20 GHz

This appendix lists dielectric properties extrapolated from the empirical equations and those from other sources where dielectric measurements were conducted in the relevant frequency ranges summarized in section 3. It provides a guide for discussion on the limitations of the empirical equations at high frequencies, as well as uncertainty assessments of computational dosimetry in relevant research fields.

Table C1. Comparison of dielectric properties of skin over 20 GHz between those extrapolated using the empirical equations by Gabriel *et al* (1996c) and those obtained by measurements.

Frequency		Gabriel *et al* (1996c)			Other sources of data	
		Skin (dry)	Skin (wet)	Dermis by Sasaki *et al* (2014, 2017)		
30 GHz	σ [S/m]	27	28	21	8.6	Skin (dry thumb) by Zhekov *et al* (2019)
	ε_r'	16	18	16	8.4	
100 GHz	σ [S/m]	39	46	47	39	Epidermis by Sasaki *et al* (2014)
	ε_r'	5.6	7.2	7.3	5.7	
300 GHz	σ [S/m]	42	56	56	55	Skin by Zaytsev *et al* (2015)
	ε_r'	4.2	4.8	4.9	3.3	
1 THz	σ [S/m]	43	65	110	55	
	ε_r'	4.0	4.2	4.5	2.6	

Table C2. Comparison of dielectric properties of adipose tissue between those extrapolated using the empirical equations by Gabriel *et al* (1996c) and those measured over 20 GHz.

Frequency		Gabriel *et al* (1996c)		Other sources of data	
		Fat (not blood infiltrated)	Fat (blood infiltrated)	Data range	Note
30 GHz	σ [S/m]	1.8	5.3	3.9–25	Tissues with high- and low-adipose contents, respectively, by Martellosio *et al* (2017)
	ε_r'	3.6	5.9	5.6–16	
100 GHz	σ [S/m]	3.6	11	20	Sasaki *et al* (2017)
	ε_r'	2.9	3.7	5.0	
300 GHz	σ [S/m]	5.1	15	14–130	Lower and higher ends are data of fat and fibers, respectively, by Ashworth *et al* (2009)
	ε_r'	2.6	2.9	2.4–3.9	
1 THz	σ [S/m]	6.8	20	40–300	
	ε_r'	2.5	2.6	2.5–3.6	

ORCID iDs

Kensuke Sasaki ⬤ https://orcid.org/0000-0002-6343-3669
Essam A Rashed ⬤ https://orcid.org/0000-0001-6571-9807
Gernot Schmid ⬤ https://orcid.org/0000-0002-3435-6844

References

Abdalla S, Al-ameer S S and Al-Magaishi S H 2010 Electrical properties with relaxation through human blood *Biomicrofluidics* **4** 034101

Abdilla L, Sammut C and Mangion L Z 2013 Dielectric properties of muscle and liver from 500 MHz–40 GHz *Electromagn. Biol. Med.* **32** 244–52

Ahad M A, Fogerson P M, Rosen G D, Narayanaswami P and Rutkove S B 2009 Electrical characteristics of rat skeletal muscle in immaturity, adulthood and after sciatic nerve injury, and their relation to muscle fiber size *Physiol. Meas.* **30** 1415–27

Ahmed M 2006 Study of the dielectric properties of breast cancer and the surrounding tissue *Egypt. J. Biophys. Biomed. Eng.* **7** 109–21

Akhtari M *et al* 2002 Conductivities of three-layer live human skull *Brain Topogr.* **14** 151–67

Alekseev S I, Gordiienko O V and Ziskin M C 2008 Reflection and penetration depth of millimeter waves in murine skin *Bioelectromagnetics* **29** 340–4

Alekseev S I and Ziskin M C 2007 Human skin permittivity determined by millimeter wave reflection measurements *Bioelectromagnetics* **28** 331–9

Alison J M and Sheppard R J 1993 Dielectric-properties of human blood at microwave-frequencies *Phys. Med. Biol.* **38** 971–8

Ashworth P C, Pickwell-MacPherson E, Provenzano E, Pinder S E, Purushotham A D, Pepper M and Wallace V P 2009 Terahertz pulsed spectroscopy of freshly excised human breast cancer *Opt. Express* **17** 12444–54

Athey T W, Stuchly M A and Stuchly S S 1982 Measurement of radio frequency permittivity of biological tissues with an open-ended coaxial line: I *IEEE Trans. Microwave Theory Tech.* **30** 82–6

Bao J Z, Lu S T and Hurt W D 1997 Complex dielectric measurements and analysis of brain tissues in the radio and microwave frequencies *IEEE Trans. Microwave Theory Tech.* **45** 1730–41

Batyuk L and Kizilova N 2018 Dielectric properties of red blood cells for cancer diagnostics and treatment *Acta Sci. Cancer Biol.* **2** 55–60

Baumann S B, Wozny D R, Kelly S K and Meno F M 1997 The electrical conductivity of human cerebrospinal fluid at body temperature *IEEE Trans. Biomed. Eng.* **44** 220–3

Berube D, Ghannouchi F M and Savard P 1996 A comparative study of four open-ended coaxial probe models for permittivity measurements of lossy dielectric biological materials at microwave frequencies *IEEE Trans. Microwave Theory Tech.* **44** 1928–34

Bi Z, Kan T, Mi C C, Zhang Y, Zhao Z and Keoleian G A 2016 A review of wireless power transfer for electric vehicles: prospects to enhance sustainable mobility *Appl. Energy* **179** 413–25

Bindu G and Mathew K T 2008 Analysis of female human breast tissues at microwave frequencies *Microwave Opt. Technol. Lett.* **50** 614–6

Brown B H, Barber D C and Seagar A D 1985 Applied potential tomography: possible clinical applications *Clin. Phys. Physiol. Meas.* **6** 109

Chahat N, Zhadobov M, Augustine R and Sauleau R 2011 Human skin permittivity models for millimetre-wave range *Electron. Lett.* **47** 427–U84

Chavez T, Vohra N, Wu J, Bailey K and El-Shenawee M 2020 Breast cancer detection with low-dimensional ordered orthogonal projection in terahertz imaging *IEEE Trans. Terahertz Sci. Technol.* **10** 176–89

Cheng Y and Fu M 2018a Dielectric properties for non-invasive detection of normal, benign, and malignant breast tissues using microwave theories *Thoracic Cancer* **9** 459–65

Cheng Y O and Fu M H 2018b Dielectric properties for differentiating normal and malignant thyroid tissues *Med. Sci. Monit.* **24** 1276–81

Chin L and Sherar M 2001 Changes in dielectric properties of *ex vivo* bovine liver at 915 MHz during heating *Phys. Med. Biol.* **46** 197–211

Chin L and Sherar M 2004 Changes in the dielectric properties of rat prostate *ex vivo* at 915 MHz during heating *Int. J. Hyperthermia* **20** 517–27

Christ A *et al* 2010 The virtual family-development of surface-based anatomical models of two adults and two children for dosimetric simulations *Phys. Med. Biol.* **55** N23–38

Dabek J, Kalogianni K, Rotgans E, van der Helm F C T, Kwakkel G, van Wegen E E H, Daffertshofer A and de Munck J C 2016 Determination of head conductivity frequency response *in vivo* with optimized EIT-EEG *Neuroimage* **127** 484–95

Dimbylow P J 1997 FDTD calculations of the whole-body averaged SAR in an anatomically realistic voxel model of the human body from 1 MHz to 1 GHz *Phys. Med. Biol.* **42** 479–90

El-Lakkani A 2001 Dielectric response of some biological tissues *Bioelectromagnetics* **22** 272–9

Ellison W 2007 Permittivity of pure water, at standard atmospheric pressure, over the frequency range 0–25 THz and the temperature range 0 °C–100 °C *J. Phys. Chem. Ref. Data* **36** 1

Farrugia L, Wismayer P S, Mangion L Z and Sammut C V 2016 Accurate *in vivo* dielectric properties of liver from 500 MHz to 40 GHz and their correlation to *ex vivo* measurements *Electromagn. Biol. Med.* **35** 365–73

Feldman Y, Puzenko A, Ben Ishai P, Caduff A, Davidovich I, Sakran F and Agranat A J 2009 The electromagnetic response of human skin in the millimetre and submillimetre wave range *Phys. Med. Biol.* **54** 3341–63

Fornes-Leal A, Garcia-Pardo C, Frasson M, Beltran V P and Cardona N 2016 Dielectric characterization of healthy and malignant colon tissues in the 0.5-18 GHz frequency band *Phys. Med. Biol.* **61** 7334–46

Foster K R and Schwan H P 1989 Dielectric properties of tissues and biological materials: a critical review *Crit. Rev. Biomed. Eng.* **17** 25–104

Foster K R and Schwan H P 1996 Dielectric properties of tissues *Handbook of Biological Effects of Electromagnetic Fields* ed C Polk and E Postow (Boca Raton: CRC Press) pp 25–102

Gabriel C 1996 Compilation of the dielectric properties of body tissues at RF and microwave frequencies *Brooks Air Force Technical Report* N. AL/OE-TR-1996-0037, Occupational and environmental health directorate, Radiofrequency Radiation Division, Brooks Air Force Base, Tex

Gabriel C 1997 Comments on 'dielectric properties of the skin' *Phys. Med. Biol.* **42** 1671–3

Gabriel C, Chan T Y A and Grant E H 1994 Admittance models for open ended coaxial probes and their place in dielectric spectroscopy *Phys. Med. Biol.* **39** 2183–200

Gabriel C and Gabriel S 1997 Compilation of the dielectric properties of body tissues at RF and microwave frequencies http://niremf.ifac.cnr.it/docs/DIELECTRIC/home.html (Accessed: November 2021)

Gabriel C, Gabriel S and Corthout E 1996a The dielectric properties of biological tissues: I. Literature survey *Phys. Med. Biol.* **41** 2231–49

Gabriel C and Peyman A 2006 Dielectric measurement: error analysis and assessment of uncertainty *Phys. Med. Biol.* **51** 6033–46

Gabriel C, Peyman A and Grant E H 2009 Electrical conductivity of tissue at frequencies below 1 MHz *Phys. Med. Biol.* **54** 4863–78

Gabriel S, Lau R W and Gabriel C 1996b The dielectric properties of biological tissues: II. Measurements in the frequency range 10 Hz to 20 GHz *Phys. Med. Biol.* **41** 2251–69

Gabriel S, Lau R W and Gabriel C 1996c The dielectric properties of biological tissues: III. Parametric models for the dielectric spectrum of tissues *Phys. Med. Biol.* **41** 2271–93

Gavazzi S, van den Berg C A T, Savenije M H F, Kok H P, de Boer P, Stalpers L J A, Lagendijk J J W, Crezee H and van Lier A 2020b Deep learning-based reconstruction of *in vivo* pelvis conductivity with a 3D patch-based convolutional neural network trained on simulated MR data *Magn. Reson. Med.* **84** 2772–87

Gavazzi S, Limone P, De Rosa G, Molinari F and Vecchi G 2018 Comparison of microwave dielectric properties of human normal, benign and malignant thyroid tissues obtained from surgeries: a preliminary study *Biomed. Phys. Eng. Express* **4** 047003

Gavazzi S, Shcherbakova Y, Bartels L W, Stalpers L J A, Lagendijk J J W, Crezee H, van den Berg C A T and van Lier A 2020a Transceive phase mapping using the PLANET method and its application for conductivity mapping in the brain *Magn. Reson. Med.* **83** 590–607

Ghanbarzadeh-Daghian A, Ahmadian M T and Ghanbarzadeh-Dagheyan A 2020 Quick, single-frequency dielectric characterization of blood samples of pediatric cancer patients by a cylindrical capacitor: pilot study *Electronics* **9** 95

Gho S M, Shin J, Kim M O and Kim D H 2016 Simultaneous quantitative mapping of conductivity and susceptibility using a double-echo ultrashort echo time sequence: example using a hematoma evolution study *Magn. Reson. Med.* **76** 214–21

Gregory A P and Clarke R N 2006 A review of RF and microwave techniques for dielectric measurements on polar liquids *IEEE Tran. Dielect. Electr. Insul.* **13** 727–43

Guardiola M, Buitrago S, Fernández-Esparrach G, O'Callaghan J, Romeu J, Cuatrecasas M, Córdova H, González Ballester M A and Camara O 2018 Dielectric properties of colon polyps, cancer, and normal mucosa: *ex vivo* measurements from 0.5 to 20 GHz *Med. Phys.* **45** 3768–82

Hirata A *et al* 2021b Assessment of human exposure to electromagnetic fields: review and future directions *IEEE Trans. Electromagn. Compat.* **63** 1619–30

Haemmerich D, Ozkan O R, Tsai J Z, Staelin S T, Tungjitkusolmun S, Mahvi D M and Webster J G 2002 Changes in electrical resistivity of swine liver after occlusion and postmortem *Med. Biol. Eng. Comput.* **40** 29–33

Haemmerich D, Schutt D J, Wright A W, Webster J G and Mahvi D M 2009 Electrical conductivity measurement of excised human metastatic liver tumours before and after thermal ablation *Physiol. Meas.* **30** 459–66

Halter R J, Schned A R, Heaney J A, Hartov A and Paulsen K D 2009 Electrical properties of prostatic tissues: I. Single frequency admittivity properties *J. Urol.* **182** 1600–7

Hampe N, Katscher U, van den Berg C A T, Tha K K and Mandija S 2020 Investigating the challenges and generalizability of deep learning brain conductivity mapping *Phys. Med. Biol.* **65** 135001

Hasgall P A, Di Gennaro F, Baumgartner C, Neufeld E, Lloyd B, Gosselin M C, Payne D, Klingenböck A and Kuster N 2015 IT'IS Database for thermal and electromagnetic parameters of biological tissues. Version 4.0, May 15, 2018. https://doi.org/10.13099/VIP21000-04-0. https://itis.swiss/database (Accessed: November 2021)

Hashimoto Y, Hirata A, Morimoto R, Aonuma S, Laakso I, Jokela K and Foster K R 2017 On the averaging area for incident power density for human exposure limits at frequencies over 6 GHz *Phys. Med. Biol.* **62** 3124–38

Henderson R P and Webster J G 1978 An impedance camera for spatially specific measurements of the thorax *IEEE Trans. Biomed. Eng.* **25** 250–4

Hirata A, Kodera S, Sasaki K, Gomez-Tames J, Laakso I, Wood A, Watanabe S and Foster K R 2021a Human exposure to radiofrequency energy above 6 GHz: review of computational dosimetry studies *Phys. Med. Biol.* **66** 135001

Huang S *et al* 2021 Differences in the dielectric properties of various benign and malignant thyroid nodules *Med. Phys.* **48** 760–9

Ibrahim F, Sayed M, H A E-G and Ghannam M 2008 Blood telomerase activity and DNA dielectric properties in human hepatocellular carcinoma and chronic liver disease *Biotechnology* **7** 66–77

Ibrahim F F and Ghannam M M 2012 The diagnostic potential of dielectric properties, telomerase activity and cytokeratin 20 in urine cells of bladder cancer patients *J. Cancer Sci. Ther.* **4** 237–42

ICNIRP 2010 Guidelines for limiting exposure to time-varying electric and magnetic fields (1 Hz to 100 kHz) *Health Phys.* **99** 818–36

ICNIRP 2020a Guidelines for limiting exposure to electromagnetic fields (100 kHz to 300 GHz) *Health Phys.* **118** 483–524

ICNIRP 2020b Gaps in knowledge relevant to the 'Guidelines for limiting exposure to time-varying electric and magnetic fields (1 Hz–100 kHz) *Health Phys.* **118** 533–42

ICRP 2002 Basic anatomical and physiological data for use in radiological protection: reference values (Annals of the ICRP) *ICRP Publication 89* vol 32 (Oxford: Pergamon)

IEEE-C95.1 2019 *IEEE Standard for Safety Levels with Respect to Human Exposure to Radio Frequency Electromagnetic Fields, 0 Hz to 300 GHz* (NY, USA: IEEE)

IFAC-CNR 1997 Internet resource for the calculation of the dielectric properties of body tissues in the frequency range 10 Hz - 100 GHz. http://niremf.ifac.cnr.it/tissprop (Accessed: November 2021)

Jacques S L 2013 Optical properties of biological tissues: a review *Phys. Med. Biol.* **58** R37–61

Jahng G H, Lee M B, Kim H J, Woo E J and Kwon O I 2021 Low-frequency dominant electrical conductivity imaging of *in vivo* human brain using high-frequency conductivity at Larmor-frequency and spherical mean diffusivity without external injection current *Neuroimage* **225** 117466

Jeong W C, Sajib S Z K, Katoch N, Kim H J, Kwon O I and Woo E J 2017 Anisotropic conductivity tensor imaging of *in vivo* canine brain using DT-MREIT *IEEE Trans. Med. Imaging* **36** 124–31

Karacolak T, Cooper R and Topsakal E 2009 Electrical properties of rat skin and design of implantable antennas for medical wireless telemetry *IEEE Trans. Antennas Propag.* **57** 2806–12

Katoch N, Choi B K, Sajib S Z K, Lee E, Kim H J, Kwon O I and Woo E J 2019 Conductivity tensor imaging of *in vivo* human brain and experimental validation using giant vesicle suspension *IEEE Trans. Med. Imaging* **38** 1569–77

Kim D H, Choi N, Gho S M, Shin J and Liu C L 2014 Simultaneous imaging of *in vivo* conductivity and susceptibility *Magn. Reson. Med.* **71** 1144–50

Kuang W and Nelson S O 1998 Low-frequency dielectric properties of biological tissues: a review with some new insights *Trans. ASABE* **41** 173–84

Kwon H, Guasch M, Nagy J A, Rutkove S B and Sanchez B 2019 New electrical impedance methods for the *in situ* measurement of the complex permittivity of anisotropic skeletal muscle using multipolar needles *Sci. Rep.* **9** 3145

La Gioia A, Porter E, Merunka I, Shahzad A, Salahuddin S, Jones M and O'Halloran M 2018 Open-ended coaxial probe technique for dielectric measurement of biological tissues: challenges and common practices *Diagnostics* **8** 40

Laakso I, Morimoto R, Heinonen J, Jokela K and Hirata A 2017 Human exposure to pulsed fields in the frequency range from 6 to 100 GHz *Phys. Med. Biol.* **62** 6980–92

Lahtinen T, Nuutinen J and Alanen E 1997 Dielectric properties of the skin *Phys. Med. Biol.* **42** 1471–2

Latikka J, Kuurne T and Eskola H 2001 Conductivity of living intracranial tissues *Phys. Med. Biol.* **46** 1611–6

Lazebnik M, Converse M C, Booske J H and Hagness S C 2006 Ultrawideband temperature-dependent dielectric properties of animal liver tissue in the microwave frequency range *Phys. Med. Biol.* **51** 1941–55

Lazebnik M *et al* 2007a A large-scale study of the ultrawideband microwave dielectric properties of normal breast tissue obtained from reduction surgeries *Phys. Med. Biol.* **52** 2637–56

Lazebnik M, Okoniewski M, Booske J H and Hagness S C 2007c Highly accurate Debye models for normal and malignant breast tissue dielectric properties at microwave frequencies *IEEE Microwave Wireless Compon. Lett.* **17** 822–4

Lazebnik M *et al* 2007b A large-scale study of the ultrawideband microwave dielectric properties of normal, benign and malignant breast tissues obtained from cancer surgeries *Phys. Med. Biol.* **52** 6093–115

Lee C, Williams J L, Lee C and Bolch W E 2005 The UF series of tomographic computational phantoms of pediatric patients *Med. Phys.* **32** 3537–48

Lee J, Shin J and Kim D-H 2016 MR-based conductivity imaging using multiple receiver coils *Magn. Reson. Med.* **76** 530–9

Lee M B, Kim H J and Kwon O I 2021 Decomposition of high-frequency electrical conductivity into extracellular and intracellular compartments based on two-compartment model using low-to-high multi-b diffusion MRI *Biomed. Eng. Online* **20** 29

Li K, Diao Y, Sasaki K, Prokop A, Poljak D, Doric V, Xi J, Kodera S, Hirata A and Hajj W E 2021 Intercomparison of calculated incident power density and temperature rise for exposure from different antennas at 10–90 GHz *IEEE Access* **9** 151654–66

Li Z *et al* 2016 A large-scale measurement of dielectric properties of normal and malignant colorectal tissues obtained from cancer surgeries at Larmor frequencies *Med. Phys.* **43** 5991–7

Li Z *et al* 2017 Variation in the dielectric properties of freshly excised colorectal cancerous tissues at different tumor stages *Bioelectromagnetics* **38** 522–32

Liebe H J, Hufford G A and Manabe T 1991 A model for the complex permittivity of water at frequencies below 1 THz *Int. J. Infrared Millimeter Waves* **12** 659–75

van Lier A, Brunner D O, Pruessmann K P, Klomp D W J, Luijten P R, Lagendijk J J W and van den Berg C A T 2012 B-1(+) Phase mapping at 7 T and its application for *in vivo* electrical conductivity mapping *Magn. Reson. Med.* **67** 552–61

Liu J, Wang Y, Katscher U and He B 2017 Electrical properties tomography based on B_1 maps in MRI: principles, applications, and challenges *IEEE Trans. Biomed. Eng.* **64** 2515–30

Lu Y J, Cui H M, Yu J and Mashimo S 1996 Dielectric properties of human fetal organ tissues at radio frequencies *Bioelectromagnetics* **17** 425–6

Mandija S, Meliado E F, Huttinga N R F, Luijten P R and van den Berg C A T 2019 Opening a new window on MR-based Electrical Properties Tomography with deep learning *Sci. Rep.* **9** 8895

Marino M, Cordero-Grande L, Mantini D and Ferrazzi G 2021 Conductivity tensor imaging of the human brain using water mapping techniques *Front. Neurosci.* **15** 694645

Martellosio A, Pasian M, Bozzi M, Perregrini L, Mazzanti A, Svelto F, Summers P E, Renne G and Bellomi M 2015 0.5–50 GHz dielectric characterisation of breast cancer tissues *Electron. Lett.* **51** 974–5

Martellosio A, Pasian M, Bozzi M, Perregrini L, Mazzanti A, Svelto F, Summers P E, Renne G, Preda L and Bellomi M 2017 Dielectric properties characterization from 0.5 to 50 GHz of breast cancer tissues *IEEE Trans. Microwave Theory Tech.* **65** 998–1011

Mayrovitz H N, Bernal M and Carson S 2012 Gender differences in facial skin dielectric constant measured at 300 MHz *Skin Res. Technol.* **18** 504–10

Mayrovitz H N, Carson S and Luis M 2010 Male-female differences in forearm skin tissue dielectric constant *Clin. Physiol. Funct. Imaging* **30** 328–32

Mayrovitz H N, Gildenberg S R, Spagna P, Killpack L and Altman D A 2018 Characterizing the tissue dielectric constant of skin basal cell cancer lesions *Skin Res. Technol.* **24** 686–91

Mayrovitz H N, Grammenos A, Corbitt K and Bartos S 2016 Young adult gender differences in forearm skin-to-fat tissue dielectric constant values measured at 300 MHz *Skin Res. Technol.* **22** 81–8

Mayrovitz H N, Mahtani S A, Pitts E and Michaelos L 2017 Race-related differences in tissue dielectric constant measured noninvasively at 300 MHz in male and female skin at multiple sites and depths *Skin Res. Technol.* **23** 471–8

Mayrovitz H N, Weingrad D N, Brlit F, Lopez L B and Desfor R 2015 Tissue dielectric constant (TDC) as an index of localized arm skin water: differences between measuring probes and genders *Lymphology* **48** 15–23

Mirabella F M 1993 *Internal Reflection Spectroscopy Theory and Applications* (New York: Marcel Dekker)

Mirbeik-Sabzevari A, Ashinoff R and Tavassolian N 2018 Ultra-wideband millimeter-wave dielectric characteristics of freshly excised normal and malignant human skin tissues *IEEE Trans. Biomed. Eng.* **65** 1320–9

Mizuno M, Kitahara H, Sasaki K, Tani M, Masami K, Suzuki Y, Tasaki T, Tatematsu Y, Fukunari M and Wake K 2021 Dielectric property measurements of corneal tissues for computational dosimetry of the eye in terahertz band *in vivo* and *in vitro Biomed. Opt. Express* **12** 1295–307

Mohammed B, Bialkowski K, Abbosh A, Mills P C and Bradley A P 2016 Dielectric properties of dog brain tissue measured *in vitro* across the 0.3-3GHz band *Bioelectromagnetics* **37** 549–56

Mosig J R, Besson J C E, Gexfabry M and Gardiol F E 1981 Reflection of an open-ended coaxial line and application to nondestructive measurement of materials *IEEE Trans. Instrum. Meas.* **30** 46–51

Nagaoka T, Kunieda E and Watanabe S 2008 Proportion-corrected scaled voxel models for Japanese children and their application to the numerical dosimetry of specific absorption rate for frequencies from 30 MHz to 3 GHz *Phys. Med. Biol.* **53** 6695–711

O'Rourke A P, Lazebnik M, Bertram J M, Converse M C, Hagness S C, Webster J G and Mahvi D M 2007 Dielectric properties of human normal, malignant and cirrhotic liver tissue: *in vivo* and *ex vivo* measurements from 0.5 to 20 GHz using a precision open-ended coaxial probe *Phys. Med. Biol.* **52** 4707–19

Pethig R 1984 Dielectric properties of biological materials: biophysical and medical applications *IEEE Trans. Electr. Insul.* **19** 453–74

Peyman A and Gabriel C 2010 Cole–Cole parameters for the dielectric properties of porcine tissues as a function of age at microwave frequencies *Phys. Med. Biol.* **55** N413–9

Peyman A and Gabriel C 2012a Dielectric properties of rat embryo and foetus as a function of gestation *Phys. Med. Biol.* **57** 2103–16

Peyman A and Gabriel C 2012b Dielectric properties of porcine glands, gonads and body fluids *Phys. Med. Biol.* **57** N339–44

Peyman A, Gabriel C, Benedickter H R and Frohlich J 2011 Dielectric properties of human placenta, umbilical cord and amniotic fluid *Phys. Med. Biol.* **56** N93–8

Peyman A, Gabriel C, Grant E H, Vermeeren G and Martens L 2009 Variation of the dielectric properties of tissues with age: the effect on the values of SAR in children when exposed to walkie-talkie devices *Phys. Med. Biol.* **54** 227–41

Peyman A, Holden S J, Watts S, Perrott R and Gabriel C 2007 Dielectric properties of porcine cerebrospinal tissues at microwave frequencies: *in vivo*, *in vitro* and systematic variation with age *Phys. Med. Biol.* **52** 2229–45

Peyman A, Kos B, Djokić M, Trotovšek B, Limbaeck-Stokin C, Serša G and Miklavčič D 2015 Variation in dielectric properties due to pathological changes in human liver *Bioelectromagnetics* **36** 603–12

Pickwell E, Cole B E, Fitzgerald A J, Pepper M and Wallace V P 2004 *In vivo* study of human skin using pulsed terahertz radiation *Phys. Med. Biol.* **49** 1595–607

Plonsey R and Barr R 1982 The four-electrode resistivity technique as applied to cardiac muscle *IEEE Trans. Biomed. Eng.* **29** 541–6

Pollacco D A, Farina L, Wismayer P S, Farrugia L and Sammut C V 2018 Characterization of the dielectric properties of biological tissues and their correlation to tissue hydration *IEEE Trans. Dielectr. Electr. Insul.* **25** 2191–7

Pop M, Molckovsky A, Chin L, Kolios M C, Jewett M A S and Sherar M 2003 Changes in dielectric properties at 460 kHz of kidney and fat during heating: importance for radio-frequency thermal therapy *Phys. Med. Biol.* **48** 2509–25

Porter E and O'Halloran M 2017 Investigation of histology region in dielectric measurements of heterogeneous tissues *IEEE Trans. Antennas Propag.* **65** 5541–52

Putzeys T, Starovoyt A, Verhaert N and Wubbenhorst M 2021 The dielectric behavior of human *ex vivo* cochlear perilymph *IEEE Trans. Dielectr. Electr. Insul.* **28** 932–7

Raicu V 1999 Dielectric dispersion of biological matter: model combining Debye-type and 'universal' responses *Phys. Rev. E* **60** 4677–80

Ranade A A, Undre P, Barpande S R, Tupkari J V and Mehrotra S C 2016 Salivary dielectric properties in oral cancer (OSCC) Through time domain reflectometry at microwave region: the future alternative for diagnosis and treatment *J. Med. Res.* **16** 13–22

Rashed E A, Diao Y L and Hirata A 2020b Learning-based estimation of dielectric properties and tissue density in head models for personalized radio-frequency dosimetry *Phys. Med. Biol.* **65** 065001

Rashed E A, Gomez-Tames J and Hirata A 2020a Deep learning-based development of personalized human head model with non-uniform conductivity for brain stimulation *IEEE Trans. Med. Imaging* **39** 2351–62

Rayes M M, Nagib G and Abdelaal W G 2016 A review on wireless power transfer *Int. J. Eng. Trends Tech.* **40** 272–80

Reilly J P and Hirata A 2016 Low-frequency electrical dosimetry: research agenda of the IEEE international committee on electromagnetic safety *Phys. Med. Biol.* **61** R138–49

Sabouni A, Mancini A, Khamechi M, Gutierrez L S and Kalter V G 2020 Determining a correction coefficient for dielectric properties between *in vivo* and *ex vivo* tumor *IEEE Trans. Dielectr. Electr. Insul.* **27** 1076–9

Sajib S Z K, Chauhan M, Kwon O I and Sadleir R J 2021 Magnetic-resonance-based measurement of electromagnetic fields and conductivity *in vivo* using single current administration-A machine learning approach *PLoS One* **16** e0254690

Sanchez B, Li J, Bragos R and Rutkove S B 2014 Differentiation of the intracellular structure of slow-versus fast-twitch muscle fibers through evaluation of the dielectric properties of tissue *Phys. Med. Biol.* **59** 2369–80

Sasaki K, Isimura Y, Fujii K, Wake K, Watanabe S, Kojima M, Suga R and Hashimoto O 2015 Dielectric property measurement of ocular tissues up to 110 GHz using 1 mm coaxial sensor *Phys. Med. Biol.* **60** 6273–88

Sasaki K, Mizuno M, Wake K and Watanabe S 2017 Monte Carlo simulations of skin exposure to electromagnetic field from 10 GHz to 1 THz *Phys. Med. Biol.* **62** 6993–7010

Sasaki K, Nishikata A, Watanabe S and Fujiwara O 2018 Intercomparison of methods for measurement of dielectric properties of biological tissues with a coaxial sensor at millimeter-wave frequencies *Phys. Med. Biol.* **63** 205008

Sasaki K, Segawa H, Mizuno M, Wake K, Watanabe S and Hashimoto O 2013 Development of the complex permittivity measurement system for high-loss biological samples using the free space method in quasi-millimeter and millimeter wave bands *Phys. Med. Biol.* **58** 1625–33

Sasaki K, Wake K and Watanabe S 2014b Development of best fit Cole-Cole parameters for measurement data from biological tissues and organs between 1 MHz and 20 GHz *Radio Sci.* **49** 459–72

Sasaki K, Wake K and Watanabe S 2014a Measurement of the dielectric properties of the epidermis and dermis at frequencies from 0.5 GHz to 110 GHz *Phys. Med. Biol.* **59** 4739–47

SCENIHR 2009 *Health Effects of Exposure to EMF* (European Commission)

SCENIHR 2015 *Potential Health Effects of Exposure to Electromagnetic Fields (EMF)* (European Commission)

Schmid G, Cecil S and Uberbacher R 2013 The role of skin conductivity in a low frequency exposure assessment for peripheral nerve tissue according to the ICNIRP 2010 guidelines *Phys. Med. Biol.* **58** 4703–16

Schmid G, Neubauer G, Illievich U M and Alesch F 2003a Dielectric properties of porcine brain tissue in the transition from life to death at frequencies from 800 to 1900 MHz *Bioelectromagnetics* **24** 413–22

Schmid G, Neubauer G and Mazal P R 2003b Dielectric properties of human brain tissue measured less than 10 h postmortem at frequencies from 800 to 2450 MHz *Bioelectromagnetics* **24** 423–30

Schmid G and Uberbacher R 2005 Age dependence of dielectric properties of bovine brain and ocular tissues in the frequency range of 400 MHz to 18 GHz *Phys. Med. Biol.* **50** 4711–20

Schmid G, Uberbacher R, Samaras T, Tschabitscher M and Mazal P R 2007 The dielectric properties of human pineal gland tissue and RF absorption due to wireless communication devices in the frequency range 400–1850 MHz *Phys. Med. Biol.* **52** 5457–68

Schmidt R and Webb A 2016 A new approach for electrical properties estimation using a global integral equation and improvements using high permittivity materials *J. Magn. Reson.* **262** 8–14

Schwan H P and Ferris C D 1968 Four-electrode null techniques for impedance measurement with high resolution *Rev. Sci. Instrum.* **39** 481–5

Schwan H P 1957 Electric al properties of tissue and cell suspensions *Advances in Biological and Medical Physics* ed J H Lawrence and C A Tobias (New York: Elsevier) pp 147–209

Shawki M M, Azmy M M, Salama M and Shawki S 2022 Mathematical and deep learning analysis based on tissue dielectric properties at low frequencies predict outcome in human breast cancer *Technol. Health Care* **30** 633–45

Shi J *et al* 2018 Automatic evaluation of traumatic brain injury based on terahertz imaging with machine learning *Opt. Express* **26** 6371–81

Shin J, Kim M J, Lee J, Nam Y, Kim M O, Choi N, Kim S and Kim D H 2015 Initial study on *in vivo* conductivity mapping of breast cancer using MRI *J. Magn. Reson. Imaging* **42** 371–8

Stoneman M R, Kosempa M, Gregory W D, Gregory C W, Marx J J, Mikkelson W, Tjoe J and Raicu V 2007 Correction of electrode polarization contributions to the dielectric properties of normal and cancerous breast tissues at audio/radiofrequencies *Phys. Med. Biol.* **52** 6589–604

Stuchly M A, Athey T W, Samaras G M and Taylor G E 1982 Measurement of radio frequency permittivity of biological tissues with an open-ended coaxial line: II. Experimental results *IEEE Trans. Microwave Theory Tech.* **30** 87–92

Stuchly M A and Stuchly S S 1980a Coaxial line reflection methods for measuring dielectric properties of biological substances at radio and microwave frequencies-a review *IEEE Trans. Instrum. Meas.* **29** 176–83

Stuchly M A and Stuchly S S 1980b Dielectric properties of biological substances — Tabulated *J. Microw. Power Electromagn. Energy* **15** 19–26

Sugitani T, Kubota S, Kuroki S, Sogo K, Arihiro K, Okada M, Kadoya T, Hide M, Oda M and Kikkawa T 2014 Complex permittivities of breast tumor tissues obtained from cancer surgeries *Appl. Phys. Lett.* **104** 253702

Sun X D, Lu L J, Qi L, Mei Y J, Liu X Y and Chen W F 2020 A robust electrical conductivity imaging method with total variation and wavelet regularization *Magn. Reson. Imaging* **69** 28–39

Sung S *et al* 2018 Optical system design for noncontact, normal incidence, THz imaging of *in vivo* human cornea *IEEE Trans. Terahertz Sci. Technol.* **8** 1–12

Tang C, You F S, Cheng G, Gao D K, Fu F and Dong X Z 2009 Modeling the frequency dependence of the electrical properties of the live human skull *Physiol. Meas.* **30** 1293–301

Tang C, You F S, Cheng G, Gao D K, Fu F, Yang G S and Dong X Z 2008 Correlation between structure and resistivity variations of the live human skull *IEEE Trans. Biomed. Eng.* **55** 2286–92

Tofighi M R and Daryoush A S 2002 Characterization of the complex permittivity of brain tissues up to 50 GHz utilizing a two-port microstrip test fixture *IEEE Trans. Microwave Theory Tech.* **50** 2217–25

Tripathi S R, Ben Ishai P and Kawase K 2018 Frequency of the resonance of the human sweat duct in a normal mode of operation *Biomed. Opt. Express* **9** 1301–8

Truong B C Q, Tuan H D, Fitzgerald A J, Wallace V P and Nguyen H T 2015 A dielectric model of human breast tissue in terahertz regime *IEEE Trans. Biomed. Eng.* **62** 699–707

Vilagosh Z, Lajevardipour A and Wood A 2019 An empirical formula for temperature adjustment of complex permittivity of human skin in the terahertz frequencies *Bioelectromagnetics* **40** 74–9

Voigt T, Katscher U and Doessel O 2011 Quantitative conductivity and permittivity imaging of the human brain using electric properties tomography *Magn. Reson. Med.* **66** 456–66

Wake K, Sasaki K and Watanabe S 2016 Conductivities of epidermis, dermis, and subcutaneous tissue at intermediate frequencies *Phys. Med. Biol.* **61** 4376–89

Wang H, He Y, Yan Q G, You F S, Fu F, Dong X Z, Shi X T and Yang M 2015 Correlation between the dielectric properties and biological activities of human *ex vivo* hepatic tissue *Phys. Med. Biol.* **60** 2603–17

Wang H, He Y, Yang M, Yan Q, You F, Fu F, Wang T, Huo X, Dong X and Shi X 2014 Dielectric properties of human liver from 10 Hz to 100 MHz: normal liver, hepatocellular carcinoma, hepatic fibrosis and liver hemangioma *Biomed. Mater. Eng.* **24** 2725–32

Watanabe A O, Ali M, Sayeed S Y B, Tummala R R and Pulugurtha M R 2021 A review of 5G front-end systems package integration *IEEE Trans. Compon. Packaging Manuf. Technol.* **11** 118–33

Wilmink G J *et al* 2011 Development of a compact terahertz time-domain spectrometer for the measurement of the optical properties of biological tissues *J. Biomed. Opt.* **16** 047006

Yamamoto T and Yamamoto Y 1976 Electrical properties of the epidermal stratum corneum *Med. Biol. Eng.* **14** 151–8

Yero D D, Gonzalez F G, Van Troyen D and Vandenbosch G A E 2018 Dielectric properties of *ex vivo* porcine liver tissue characterized at frequencies between 5 and 500 kHz when heated at different rates *IEEE Trans. Biomed. Eng.* **65** 2560–8

Yu X F, Sun Y, Cai K C, Yu H F, Zhou D F, Lu D and Xin S X 2020 Dielectric properties of normal and metastatic lymph nodes *ex vivo* from lung cancer surgeries *Bioelectromagnetics* **41** 148–55

Zaytsev K I, Kudrin K G, Karasik V E, Reshetov I V and Yurchenko S O 2015 *In vivo* terahertz spectroscopy of pigmentary skin nevi: pilot study of non-invasive early diagnosis of dysplasia *Appl. Phys. Lett.* **106** 053702

Zhang X, Liu J and He B 2014 Magnetic-resonance-based electrical properties tomography: a review *IEEE Rev. Biomed. Eng.* **7** 87–96

Zhekov S S, Franek O and Pedersen G F 2019 Dielectric properties of human hand tissue for handheld devices testing *IEEE Access* **7** 61949–59

Zurbuchen U, Holmer C, Lehmann K S, Stein T, Roggan A, Seifarth C, Buhr H J and Ritz J P 2010 Determination of the temperature-dependent electric conductivity of liver tissue *ex vivo* and *in vivo*: importance for therapy planning for the radiofrequency ablation of liver tumours *Int. J. Hyperthermia* **26** 26–33